2009

Expression of Chemokines and VEGFs in HNSCC

Crystal Cunningham
Virginia Commonwealth University

Expression of Chemokines and VEGFs in HNSCC

A thesis submitted in partial fulfillment of the requirements for the degree of Masters of Science in Biochemistry at Virginia Commonwealth University.

by

CRYSTAL CUNNINGHAM
University of Virginia, B.S. Chemistry, 2007

Director: DR. HIROSHI MIYAZAKI
PHILIPS INSTITUTE, VCU SCHOOL OF DENTISTRY

Virginia Commonwealth University
Richmond, VA
May 2009

Acknowledgement

I first would like to thank my PI, Hiroshi Miyazaki, for his continuous help and support throughout this year. Being a new laboratory student and him a first time PI, this year has been full of challenges and learning experiences for all. I would also like to thank Dr. Andrew Yeudall for use of many of his resources and knowledgeable experience. To my fellow students in lab, especially Huixin Wang, who always was able to answer questions and explain experiments. I also appreciate my committee members, Dr. Sumitra Deb and Dr. Zendra Zehner, for their time, which without this would not be possible. Finally, my lab partner Banks Allen. Without him I would not have survived throughout the year. He is always there to make everyday entertaining, listen to my frustrations, and offer his straight forward, often correct, advice.

Table of Contents

List of Tables

Page

List of Figures

Page

List of Abbreviations

DC	Dendritic Cells
EGF	Epidermal Growth Factor
EGFR	Epidermal Growth Factor Receptor
EMT	Epithelial to Mesenchymal Transition
FGF	Fibroblast Growth Factor
GAP	GTPase Activating Protein
GEF	Guanine Nucleotide Exchange Factor
GPCR	G-Protein Coupled Receptors
HGF	Hepatocyte Growth Factor
HIF	Hypoxia Inducible Factor
HNSCC	Head and Neck Squamous Cell Carcinoma
HRE	Hypoxia Response Element
IGF	Insulin-like Growth Factor
QOL	Quality of Life
MMP	Matrix Metalloproteinases
PDGF	Platelet Derived Growth Factor
RTK	Receptor Tyrosine Kinase
TAM	Tumor Associated Macrophages
TGF-β	Transforming Growth Factor β
VEGF	Vascular Endothelial Growth Factor
VEGFR	Vascular Endothelial Growth Factor Receptor
VHL	Von Hippel-Lindau

Abstract

Expression of Chemokines and VEGFs in HNSCC

A thesis submitted in partial fulfillment of the requirements for the degree of Masters of Science in Biochemistry at Virginia Commonwealth University.

by

CRYSTAL CUNNINGHAM
University of Virginia, B.S. Chemistry, 2007

Director: DR. HIROSHI MIYAZAKI
PHILIPS INSTITUTE, VCU SCHOOL OF DENTISTRY

Head and neck squamous cell carcinoma (HNSCC) is the sixth most common malignancy worldwide. The 5-year survival rate when the cancer remains as a primary tumor is 81% but when it metastasizes to distant sites, defined as a metastatic cancer, it decreases dramatically to 26%. Approaches to prevent these cancers from undergoing these metastatic changes can greatly improve the survival and outcome of these cancer victims. This current study is examining the expression profiles of chemokines and VEGFs in HNSCC. By investigation the underlying pathways involved in the expressions of chemokines and VEGFS we hope to sort out the transcriptional regulation

of these molecules. We used pharmological inhibitors of several important kinase pathways and the receptors involved in the transcription of chemokines and VEGFs. This study specifically looked at the proangiogenetic chemokines, CXCL5 and CXCL8, and their receptor CXCR2, and their possible impact on VEGFs, specifically VEGF-C and VEGF-A. From experimentation we concluded that HNSCC uses the MAPK pathway for regulation of the chemokines CXCL5 and CXCL8, but not for its downregulation. VEGF-A showed to be positively controlled by the MAPK pathway. The Akt pathway was found to downregulate VEGF-C, possibly from CXCR2. VEGF-C was not under control of the chemokines' expression, VEGF-C and VEGF-A were also differentially regulated. The current study has begun to sort out the expression and regulation of chemokines and VEGFs in HNSCC. There are still many unanswered questions about the role these molecules play in HNSCC, but hopefully these conclusions will aid in finding improved treatments for patients diagnosed with head and neck cancer.

Introduction and Background

1.1 Cancer

Cancer is a complex disease characterized by uncontrolled cell proliferation, microenvironmental changes and frequent metastasis. In the United States cancer is the second most frequent cause of death. It is predicted in 2008 that 565,650 Americans will die from cancer, equaling to more than 1,500 people per day (Cancer Facts and Figures 2007, American Cancer Society). Even with today's advanced technology it is still difficult to predict precisely who will be a cancer victim. Cells can acquire oncogenetic character due to external environmental factors, such as UV light, tobacco smoking and alcohol drinking, or innate genetic factors originally present in a patient (McMahon 2003). Mutations in two classes of genes, proto-oncogenes and tumor-suppressor genes, have been shown repeatedly to cause the onset of cancer. Proto-oncogenes normally promote cell growth, but convert their character to oncogenes by introducing constitutively active mutations on their genes. Tumor suppressor genes typically restrict abnormal cell growth, therefore mutations in these genes allow for inappropriate cell division (Lodish 2008). A few examples of these innate genetic mutations include; Von Hippel-Lindau (VHL) disease, due to mutation in the VHL gene, (Richards 1998), Beckwith-Wiedemann syndrome, due to paternal duplication in chromosome 11p15 (South 2008), and Li-Fraumeni syndrome, due to mutation in TP53 or CHEK2 genes (Ruijs 2009). The most frequent abnormality in human tumors is a mutation in p53, a tumor suppressor protein (Deb 2003). Cancer cells do not behave as normal cells. They lose their contact inhibition and acquire the ability to leave their primary site and relocate to a secondary or distant site(s). Cancer cells at secondary sites frequently demonstrate

uncontrolled proliferation, which suggests the acquisition of modified molecular profiles from the primary tumor. Once a patient is diagnosed with a certain type of cancer, the patient is treated following diagnostic indexes. The diagnostic index takes into account the location of the primary tumor, the tumor's size, the number of tumors, whether it presents invasion into the lymph nodes, the cell type, and the presence or absence of metastasis (National Cancer Institute 2009). For this classification of malignant tumors, the TNM system is a commonly used for standardizing the stages. It summarizes the size or extent of the tumor (T), and degree of spreading to the lymph nodes (N), and the presence of metastasis (M). The treatment and outcome of a cancer are usually predicted using this staging system, with early stages leading to better treatment, in general. Current standard treatments include radiation therapy and surgery (McMahon 2003). Drug therapy is also used to treat many types of cancers, targeting several different molecular mechanisms essential to cancer development. Drug therapy targets processes such as angiogenesis with vascular endothelial growth factor (VEGF) antibody, Bevacizumab, an inhibitor of receptor tyrosine kinases called Imatinib, and mitotic cellular activity, using a microtubule stabilizer, Paclitaxel. These treatments however can be life altering and frequently causes serve side effects to patients. In most cases early detection and diagnosis can greatly improve the outcome and treatments for cancer patients.

1.2 Head and Neck Cancer

Cancer that is found in the head and neck region, including the nasal cavity, sinuses, lips, mouth, salivary glands, pharynx and/or larynx is classified as head and neck

cancer. Generally more than 90% of these cancer cells arise in the mucosal surfaces, therefore are referred to as squamous cell carcinomas, or Head and Neck Squamous Cell Carcinomas (HNSCC) (National Cancer Institute 2009). Today it is almost impossible to predict who will develop head and neck cancer, but there are several major risk factors that dramatically increase the chance of cancer development. These risk factors include tobacco smoking, alcohol drinking, exposure to the sun or UV light and/or a family history of cancer development. It is statistically clear that longer periods of habitual tobacco smoking and alcohol drinking synergistically raises the risk of cancer development in the head and neck (McMahon 2003). The risk of developing HNSCC is 20 times higher among alcohol and tobacco users versus non-smokers and non-drinkers (McMahon 2003). HNSCC is the sixth most common malignancy in the developed world, and accounts for 3 to 5 percent of all cancer in the United States (National Cancer Institute 2009). There are approximately 35,000 new cases of head and neck cancer annually in the United States (American Cancer Society 2007). The 5-year survival rate when the cancer remains as a primary tumor is 81% but when it metastasizes to distant sites, defined as a metastatic cancer, it decreases dramatically to 26%. A patient's death usually occurs as a result of local invasion as well as systemic metastatic spread of the tumor cells (Miyazaki 2006). Current treatments for HNSCC include surgery, radiation therapy, and chemotherapy. These treatments are generally harsh and many times cause cosmetic, neuronal and functional problems in patients' daily life and causing impairment to their quality of life (QOL). Thus, we need to address the early detection of cancer and improve the outcome of treatments to help these patients live more enjoyable lives.

1.3 Metastasis

Metastasis is the uncontrolled spreading of cancer cells from a primary location to a distant location(s). In order for the cancer cells to undergo metastasis they must undergo a series of biological changes induced by atypical molecular expression profiles. First, they must detach from the primary site, then invade the lymphatic or circulatory system, then transport through the vessels, next attach to the inner wall of the vessel and exit the vessel at the secondary site and finally the cells have to survive at the distant site to establish metastasized colonies. As mentioned above in order to undergo these sequential changes, the cells must modify their own biological character. The transition in which these cells undergo is referred to as epithelial to mesenchymal transition or EMT. During this transition generally cells change their morphology from round in shape to spindle. They also dissolve their cell-cell junction, and as a result the cells become individual, non-polarized, motile, and invasive mesenchymal cells (Singh 2007). Along with these phenotypic changes, the expression of E-cadherin is also decreased, and N-cadherin will be upregulated, known as a cadherin switch. A number of extrinsic signals such as transforming growth factor-β (TGF-β), hepatocyte growth factor (HGF), epidermal growth factor (EGF), insulin-like growth factor (IGF), and fibroblast growth factor (FGF) also play an important role in inducing EMT (Singh 2007). These molecular signals, involved in EMT, have been shown to be upregulated in certain metastatic cell lines, versus primary cell lines (Miyazaki 2007). The differences between primary and metastatic cell lines have been explored to dissect signaling pathways and regulation involved in EMT.

1.4 Chemokines

Chemokines are known as key regulators in cell migration. It has been shown that chemokines are involved in the progression of tumor development, serving as chemoattractants in cell migration, aid in shaping the tumor's environment, and ensure survival and proliferation for metastasized cells (O'Hayre 2008). Chemokines can elicit cell movement by inducing changes in cytoskeletal structure and dynamics, as well as by directly activating growth and proliferation pathways (O'Hayre 2008). Chemokines transduce their signal through G-protein coupled receptors (GPCRs), which are also known as seven transmembrane domain receptors. These groups of receptors are well known as a major target of drugs currently available. The receptors expression level is regulated at the transcriptional level and as well as through post-transcriptional modification (O'Hayre 2008). Recently, it has been shown that specific chemokine receptor expression is responsible for directing organ specific metastasis (Muller 2001). Through these important observations it is suggested that receptors present on the surface of migratory cancer cells are targeted to ligands present on cells at the site of metastasis (Muller 2001). So far, there are about 50 human chemokines and 20 chemokines receptors known and characterized (O'Hayre 2008). These chemokines are categorized into four major families, which are C, CC, CXC and CX_3C (Figure 1). This classification is based on the distribution of cysteine (C) residues at the C terminus end, where X represents any amino acid. It is well known that the family of CXC chemokines plays a critical role in angiogenesis (Mehrad 2007). This family of CXC chemokines can be further sub-divided into two groups depending on whether they contain glutamine-leucine-arginine, or ELR(+), or not, ELR(-). This ELR sequence is present at the N-

terminus immediately before the first cysteine amino acid residue (Singh 2007). ELR(+) CXC chemokines are functionally categorized as chemoattractants and angiogenic promoters, while ELR(-) CXC chemokines are defined angiostatic. The only exception to this rule is CXCL12, which is an ELR(-) CXC chemokine but has been shown to function as an angiogenic chemokine. Chemokines elicit their functions through binding to a number of G protein coupled receptors (GPCRs). The activation of GPCRs sequentially induces activation of a number of intracellular signaling pathways such as Akt, Erk1/2 and NFκB, which leads to transcription of specific targeted genes for cell survival, proliferation and cell cycle promoting genes (O'Hayre 2008). However, these signaling pathways are complex and often are cell dependent. Additional organ and/or tissue specific knowledge involved in these pathways may help in developing therapeutic measures to combat metastasis, and more advanced stages of cancer. By analyzing the angiogenic promoting signals, we may have a chance to downregulate the growth of microvessels, which provide oxygen, and many additional growth factors to the primary and metastatic solid tumors. This can be a therapeutic approach to treat advanced stages of primary and/or metastasis solid tumors. For this purpose several drugs are now under development and a limited numbers of drugs are clinically applied for these angiogenesis rich tumors, but highly specific drugs that target only abnormal vessels, have been long awaited.

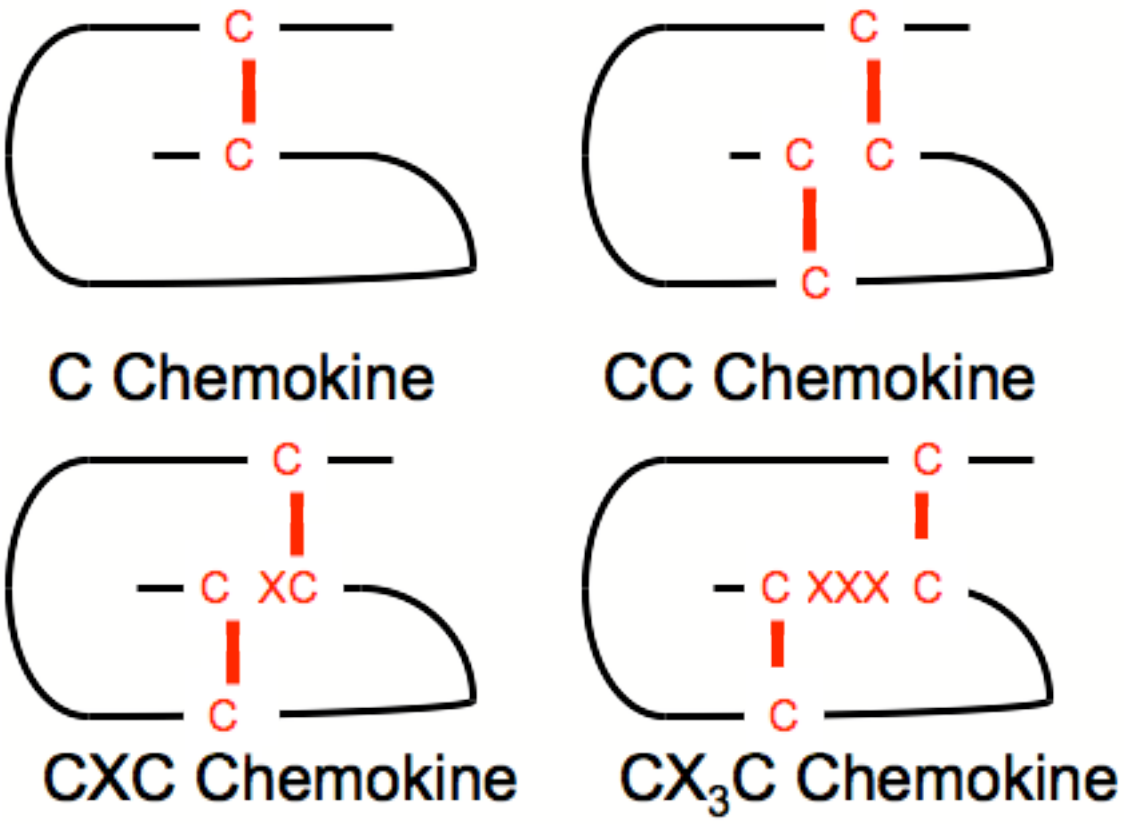

Figure. 1 Structure of the four classes of chemokines. C residues are cysteine, and X is any amino acid. The cysteine residues are connected by disulfide bonds.

1.5 CXC chemokine CXCL5 and CXCL8

CXCL5 and CXCL8 (also known as IL-8) are ELR(+) CXC chemokines and are known as representative pro-inflammatory chemokines. CXCL8 has been found to bind both CXCR1 and CXCR2, while CXCL5 binds exclusively to CXCR2. CXCL8 expression is well known to promote angiogenesis, allowing for proliferation, cell survival, and migration of endothelial cells (Waugh 2008). CXCL5 has also been shown to be involved in similar processes, such as tumor cell proliferation, invasion and migration (Miyazaki 2006). Previously our lab performed cDNA microarrays, using cDNAs derived from the HN4 primary cell line and HN12 metastatic cell lines in order to identify target genes that are differentially expressed between them. These cell lines are derived from one male patient, the HN4 cell line from a cancer of the tongue and HN12 cell line from the nodal metastasis site. These experiments showed an increased level of transcribed mRNA in CXCL5 7.3 fold and a 2.2 fold increase in CXCL8, in the HN12 cell line versus HN4 (Miyazaki 2006). Pre-treating the metastatic HNSCC cell line HN12 with EGF made this effect more profound, leading to an 18.5 fold upregulation in CXCL5 expression (Miyazaki 2006). Western blot analysis further supported that HN12 cells secrete CXCL5 clearly, but was undetectable in HN4 cells (Miyazaki 2006). Downregulation of CXCL5 using retroviral vector based shRNA system in the HN12 cell line exhibited decreased migration as well as downregulated tumorigenicity as compared to the wild type (Miyazaki 2006). RNAi-mediated knockdown of CXCL8 expression in HN12, which normally expresses high levels of CXCL8, showed decreased proliferation as well (Christofakis 2007). CXCL8 has been found to upregulate proliferation and promote chemotaxis of endothelial cells (Schruefer 2005). It has been suggested that

these CXCL8 role can be induced through the activation of MAPK, PI-3K and p38 MAP kinase signaling cascades (Waugh 2008). CXCL8 has also been shown to induce phosphorylation of vascular endothelial growth factor receptor-2 (VEGFR-2) in endothelial cells (Patreaca 2007). In summary, these two ELR (+) chemokines have been found repeatedly to play a critical role in promoting metastasis through their biological effect on tumor cells.

1.6 G-protein Coupled Receptors (GPCRs)

Chemokines are known to bind and transduce their signal through GPCRs. All GPCR pathways consist of a receptor that contains a seven transmembrane domain, a coupled trimeric G-protein subunit that alternates between an active and inactive form, a membrane bound effector protein, and a feedback regulation and desensitization pathway (Lodish 2008). These receptors have their N-terminus outside the cell membrane, three extracellular and three intracellular loops spanning the cell membrane, and a C-terminus containing serine and threonine phosphorylation sites present in the cytosol (Singh 2007). Trimeric G-proteins consist of three subunits, α, β, and γ. During signaling, G_β and G_γ subunits stay bound together, and together they are called the $G_{\beta\gamma}$ subunit. The α subunit, referred to as the G_α subunit, is in the resting state when it is bound with GDP (Guanosine-5'-diphosphate) and is attached to the $G_{\beta\gamma}$ subunit. Upon binding of a ligand to the G-protein receptor, the receptor undergoes a conformational change, allowing the G_α subunit to release GDP and bind GTP (Guanosine-5'-triphosphate). Guanine nucleotide-exchange factor (GEF) catalyzes the dissociation of GDP and allowing GTP to bind (Lodish 2008). The G_α-GTP can then interact with other effector proteins (Lodish

2008) (Figure 2). This activity is short lived, a bound GTP gets hydrolyzed to GDP in minutes, inactivating the signal. The conversion of active G_α-GTP into inactive G_α-GDP is accelerated by GTPase-activating proteins (GAP) (Lodish 2008). Chemokines bind to a variety of these GPCRs, with some specific combinations and some overlap. Different classes of chemokines have their own receptors (Table 1). There are six CXC receptors currently known (Singh 2007). CXCR1 has been shown to bind CXCL8 with high affinity, while CXCR2 has been shown to bind all ELR(+) CXC chemokines with high affinity (Singh 2007). The CXCR1 and CXCR2 share 78% identity in their amino acid sequence, and vary mostly in the amino terminus, carboxyl terminus and second extracellular loop (Addison 2000). ELR(-) chemokines bind to CXCR3, resulting in angiostatic responses. GPCRs can be divided into classes based on their G_α subunit. Examples of the classes of GPCR include G_s, G_i, G_{olf}, G_q, G_o, and G_t (Lodish 2008). These CXC receptors belong to the G_i family. These G_i receptors inhibit the activity of adenylyl cyclases, leading to the reduction of the intracellular cAMP (cyclic adenosine monophosphate) concentration (Piiper 2004). Changes in the amount of cAMP in turn effects adenylyl cyclase, and further associate proteins. As mentioned above, GPCRs are a large family of receptors that signal upon ligand binding through the G_α subunit to a number of signaling pathways to elicit their downstream effects. However, these downstream signaling events are complex and still need to be elucidated further.

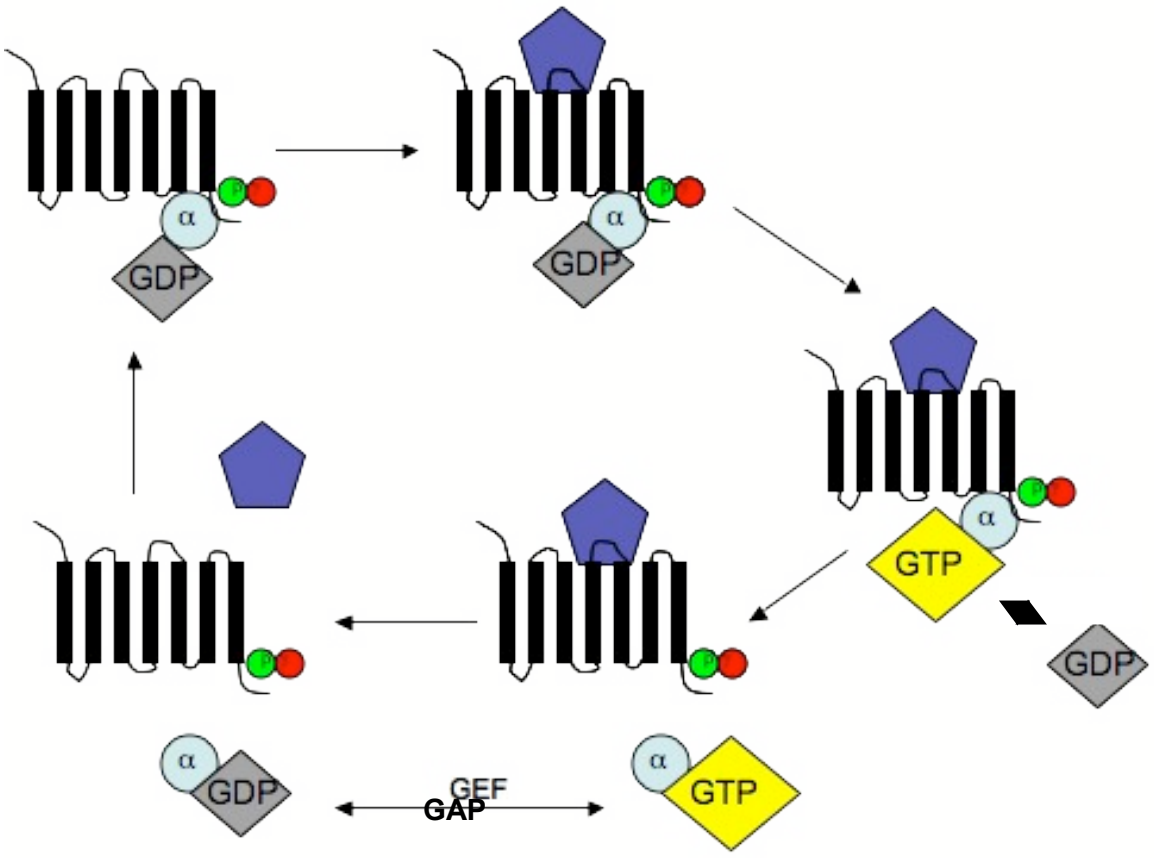

Figure 2. G-Protein coupled receptor activation scheme.

Chemokine Receptors	Ligands	Tumorgenic Properties
CXCR1/2	CXCL1, 2, 3, 5, 6, 7, and 8	Angiogenesis, invasion and metastasis, growth and proliferation, survival, MMP-2/9/ MT1-MMP expression
CXCR3	CXCL9, 10, and 11	Invasion and metastasis, survival, proliferation
CXCR4	CXCL12	Angiogenesis, invasion and metastasis, growth and proliferation, survival, DC recruitment, MMP-9 expression
CXCR5	CXCL13	Invasion and metastasis, growth and proliferation
CXCR7	CXCL12	Growth, survival
CCR1	CCL3, 4, 5, 7, 16 and 23	TAM and DC recruitment, polarization, invasion and metastasis, angiogenesis, MMP9/19 expression
CCR2	CCL2, 7, 8, 12	TAM and fibroblast recruitment, polarization, invasion and metastasis, angiogenesis, MMP-12/MT1-MMP expression
CCR3	CCL5, 7, 11, 24 and 26	TAM and esoinophil recruitment, invasion and metastasis, angiogenesis, angiogenesis, MMP-19 expression
CCR4	CCL2, 3, 5, 17 and 22	TAM and T-cell recruitment, invasion and metastasis
CCR5	CCL3, 4, 5 and 8	TAM recruitment, polarization, invasion and metastasis, growth, MMP-19 expression
CCR6	CCL20	DC recruitment, invasion and metastasis, proliferation
CCR7	CCL19, 21	Invasion and metastasis, survival
CCR9	CCL25	Invasion and metastasis, survival
CCR10	CCL27	Invasion and metastasis, growth, survival
CX3CR1	CX3CL1	Invasion and metastasis, survival

Table 1. Pro-tumorgenic chemokines and receptors (O'Hayre 2008).

1.7 Vascular Endothelial Growth Factors (VEGFs)

Tumors require the recruitment or development of new blood vessels in the tumor's surrounding area to grow into a larger mass. Angiogenesis is the process in which tumors induce formation of new blood vessels to nourish the growing tumor. Vascular Endothelial Growth Factors (VEGFs) have been shown to be pro-angiogenic and pro-tumorigenic (Tong 2008). VEGFs belong to the platelet derived growth factor (PDGF) family, and exist as disulfide-linked dimeric glycoproteins with molecular weight ranges from 34 to 43 kDa (Ninck 2003). Five genes are known to be responsible for encoding VEGF families. They are identified as VEGF-A, -B, -C, -D, and -E. Each of these independent isoforms is generated from different alternative splicing variants (Neuchrist 2003). VEGF-A and VEGF-C have both been shown to play a critical role in tumor development (George 2001). Neoangiogenesis is the formation of new capillaries from pre-existing blood vessels, which is required when tumors grow bigger than 2 to 3 mm^3 in volume (George 2001). This phenomenon is promoted by angiogenic cytokines, such as VEGFs. VEGF-A promotes angiogenesis. VEGF-A can exist in multiple splicing variants, $VEGF_{165}$ being one of the dominantly expressed isoforms of VEGF-A, and it functions as a chemoattractant for endothelial cells and increases permeability of blood vessel permeability (Ninck 2003). VEGF-C on the other hand has been shown to be involved in vascular and lymphangiogenesis in HNSCC (Neuchrist 2003). The transcription levels of VEGFs are negatively regulated by the amount of oxygen available to the cell. When cells become deprived of oxygen they induce transcription of hypoxia-inducible factor (HIF-1), which increases the formation of blood vessels (Martin 2009). HIF-1 is composed of two subunits, HIF-1α and HIF-1β. Under hypoxic conditions,

HIF-1α translocates to the nucleus and binds to HIF-1β, where it binds to hypoxia responsive elements (HRE) and induces transcription of certain genes, such as these VEGFs, especially VEGF-A and VEGF-C (Martin 2009). VEGFs must be transcribed in order to provide a blood supply to the tumor. Without the assistance of these VEGFs the tumor would not be able to continue to proliferate and survive.

	Receptor	Chromosome Location	Principle Roles	Isoforms
VEGF-A	VEGFR-1 VEGFR-2 VEGFR-3	6p12	Angiogenesis, Chemotactic for macrophages and granulocytes, Vasodilatation	$VEGF_{206}$ isoform a $VEGF_{189}$ isoform b $VEGF_{183}$ isoform c $VEGF_{165}$ isoform d $VEGF_{148}$ isoform e $VEGF_{121}$ isoform f $VEGF_{165b}$ isoform g
VEGF-B	VEGFR-1	11q13	Embryonic angiogenesis	
VEGF-C	VEGFR-2 VEGFR-3	4q34.1-34.3	Lymphangiogenesis	
VEGF-D	VEGFR-2 VEGFR-3	Xp22.31	Lymphatic surrounding lung bronchioles	
VEGF-E	VEGFR-2	Recombinant of Orf virus	Angiogenesis during ischemia, inflammation, wound healing	

Table 2. Summary table of VEGF isoforms, their receptors, chromosome location, principle roles and various isoforms.

1.8 Receptor Tyrosine Kinases (RTKs)

Receptor Tyrosine Kinases (RTKs) are a class of cell-surface receptors. Soluble or membrane bound proteins activate these RTKs. VEGFs bind to these RTKs and elicit their downstream response. In the absence of ligands RTKs exist as monomers with poor kinase activity. In the presence of ligands, the receptor undergoes a conformational change, forming a dimeric receptor that can phosphorylate each other in the activation lip. The phosphorylation causes the lip to move out of the catalytic site, allowing ATP or a protein to bind. The kinase then self phosphorylates other tyrosine residues in the cytosolic domain on receptors. In this event the phosphorylated tyrosines, function as docking sites for other signaling molecules (Lodish 2008). There are two ways in which to downregulate the RTKs signal. First, the ligand can induce endocytosis of the receptor-ligand complex, reducing the firing number. Second, the receptor or ligand independently can be internalized and sorted to the lysosome for degradation (Lodish 2008). Currently there are three known RTKs that have been identified for VEGFs, VEGFR-1, VEGFR-2, and VEGFR-3 (Tong 2008). VEGFR-2 is considered as a dominant mediator of mitogenesis in epithelial cells (Tong 2008). Each VEGF can signal through one or multiple VEGFRs (Table 2). Binding of VEGF to the receptor, and its downstream signaling is an indispensable process in angiogenesis. This signaling event through VEGFR leads to increased microvessel density (Tong 2008). Inducing transcription of the VEGFs allows the tumor to grow larger than 2 to 3 mm^3 in volume. The increase in number in blood vessels provides the tumor with an increased amount of nutrients and efficient waste removal to allow for its continued growth. Thus downregulation of the transcription and signaling activity of these VEGF pathways could

decrease the tumor's potential to proliferate. Some antagonist, such as angiogenin and endostain, of the VEGF receptor are currently being applied for angiogenic rich tumors as a molecular based therapeutic approach (Lodish 2008). Additional research needs to be done to sort out combination as well as new treatments in order to reduce tumor proliferation for anti-VEGF (or anti-VEGFR) based therapy.

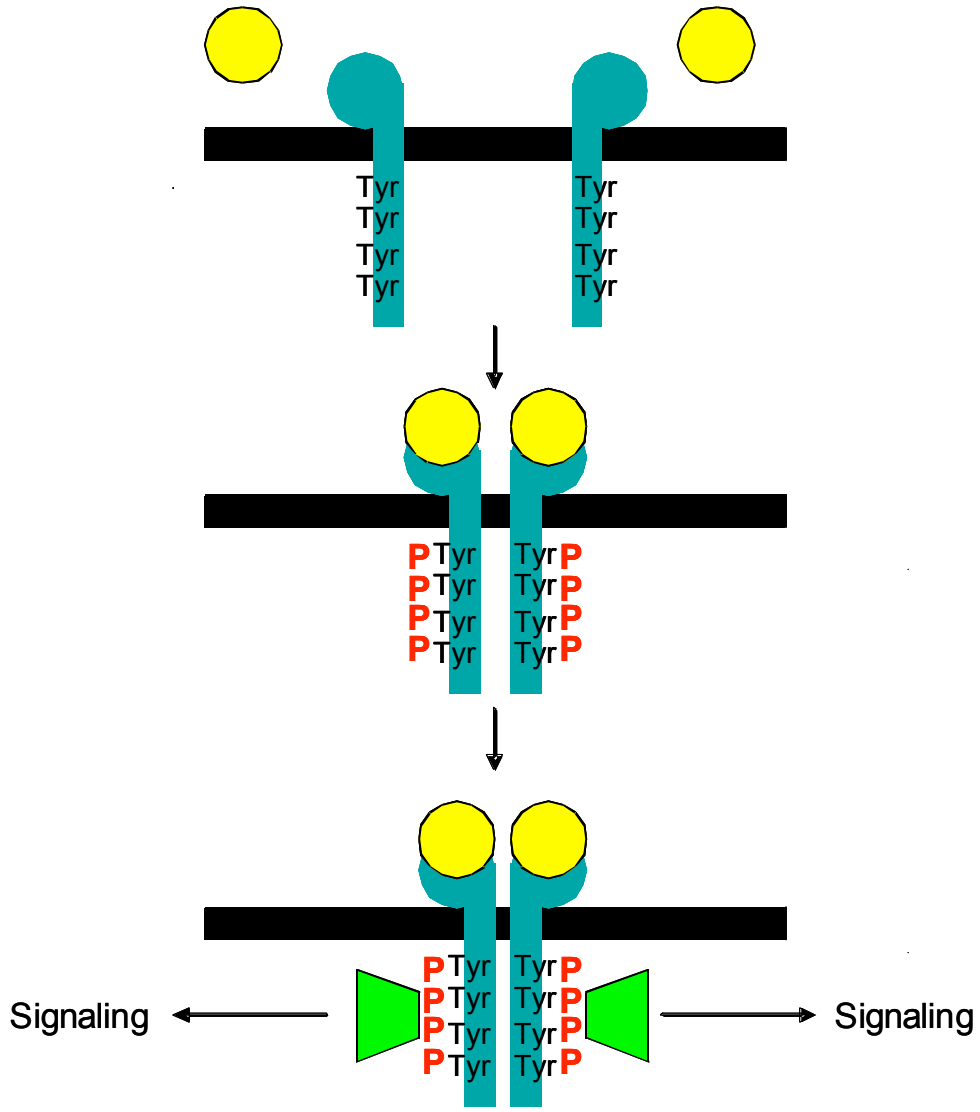

Figure 3. Receptor tyrosine kinases (RTKs) activation scheme

1.9 Crosstalk between GPCR and RTK

It has been shown in the previous research that GPCRs and RTKs activate a common set of signaling molecules that do not operate in an independent fashion (Delcourt 2007). There is crosstalk that occurs between GPCR and RTK, which is most commonly referred to as transactivation. Two modes of transactivation have been identified, the first being ligand dependent and the other, ligand independent (Delcourt 2007). Ligand dependent mode involves activation of GPCR, which then causes production of a transmembrane RTK ligand precursor (Delcourt 2007). Ligand independent mode involves activation of the cross communication of the GPCR and RTK by a protein complex or phosphorylation downstream of the receptor (Delcourt 2007). GPCRs can use RTKs in order to mediate downstream signaling (Piiper 2004). An example of this occurring is IGF-1, which transactivates the CXCR4, a G_i receptor, in metastatic cancer epithelial cells independently of CXCL12 (Delcourt 2007). Another example is seen with Epidermal Growth Factor (EGF). EGF and its receptor, epidermal growth factor receptor (EGFR), a RTK, have been found to be upregulated in HNSCC. Interactions between these EGFR and GPCRs can result in a more aggressive tumor phenotype (Thomas 2006). The downstream signaling pathways of chemokines / GPCRs and VEGFs / RTKs contain overlapping molecules (Figure 4, 5). It is possible that there is crosstalk transactivating between these two thought to be independent pathways. Recently the observation using Human Umbilical Vein Endothelial Cells (HUVEC) revealed that upregulation of VEGF-C, was almost completely inhibited by applying CXCL8 antibody (Schruefer 2005). The similarity between chemokines signaling pathway and VEGF signaling pathway suggests that there could be possible crosstalk

between these two signaling pathways.

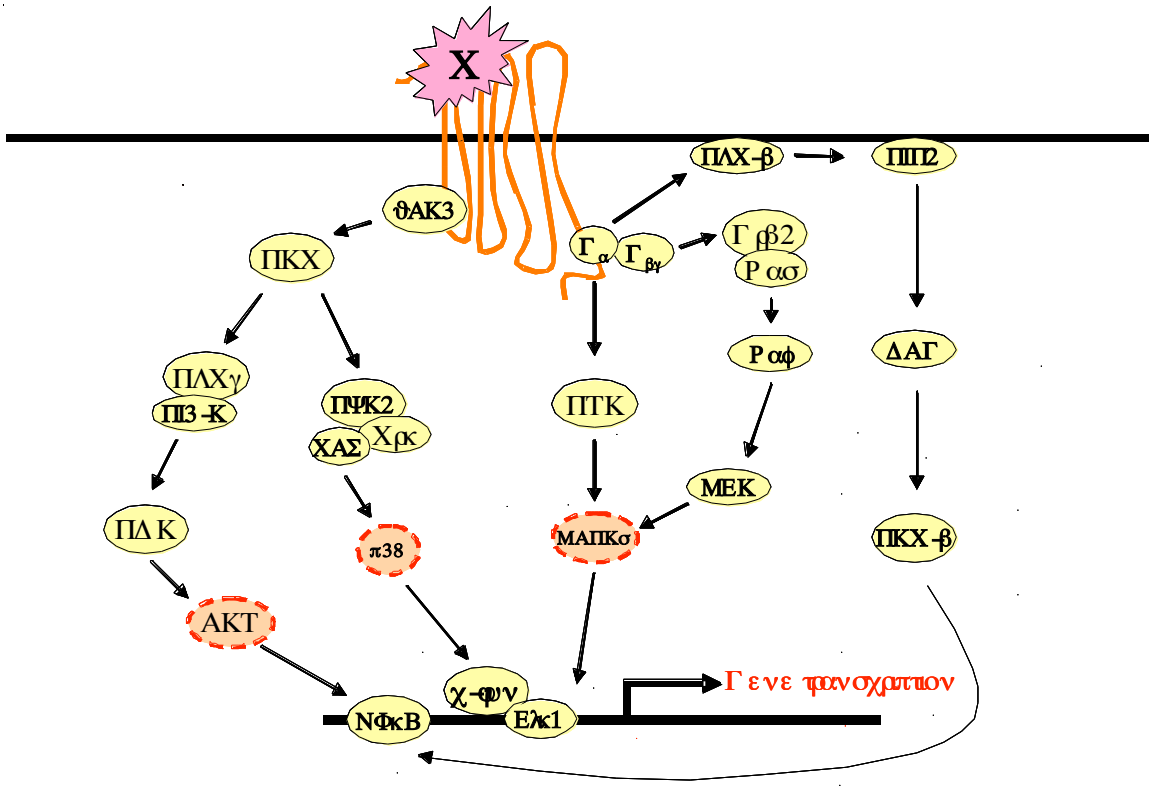

Figure 4. Known chemokines signaling pathway.

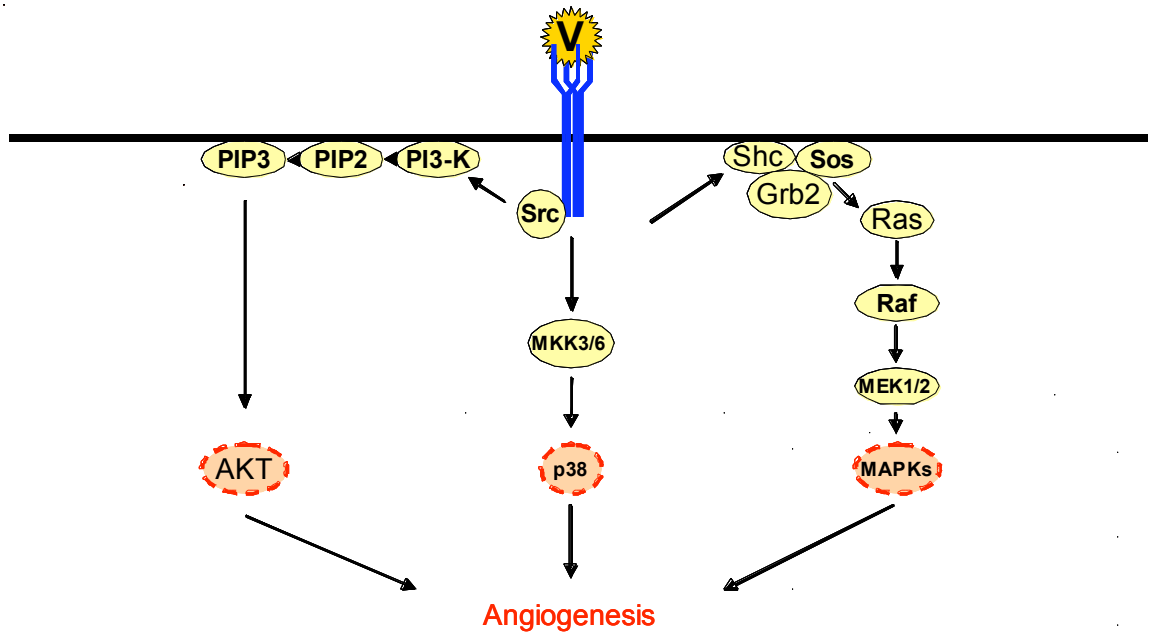

Figure 5. Known VEGFs signaling pathway.

Material and Methods

2.1 Cell Culture

Head and neck squamous cell carcinoma (HNSCC) cell lines HN4 and HN12, were cultured in Dulbecco's Modified Eagle Medium (D-MEM) (Mediatech, Manassas, VA), with 10% Serum Supreme (SS) (Lonza, Walkersville, MD) and 1 ml of 100 U/mL penicillin / 100 μg/mL streptomycin (Mediatech, Manassas, VA) per 100 mL. The cell lines were maintained in an incubator at 37°C, with 90% air and 10% CO_2.

2.2 Cell Proliferation Assay

HN4 and HN12 cells were cultured in 24 well culture plates (Greiner Bio-One, Monroe, NC). The originally plated HN4 and HN12 were matched to contain $5x10^3$ cells. Both cell lines were cultured in a 37°C incubator, with 90% air and 10% CO_2. Cells were cultured with either 10% SS containing D-MEM, or with 10% SS contained D-MEM with DMSO (Dimethyl sulfoxide), or 10% SS contained D-MEM in the presence of inhibitors. Cells were counted everyday by removing medium, washing once with phosphate buffered saline (PBS) and trypsinized by adding 300μL of trypsin per well and placed for 20 minutes in the 37°C, 90% air and 10% CO_2 incubator. Cells were knocked loose and completely resuspended by pipetting in the trypsin. 20 μL of the resuspended cells were then applied to the Improved Neubauer Haemocytometer. Four independent wells were counted per day, averaged, and standard deviation (SD) was calculated on each averaged number.

2.3 RNA Extraction

Cells were cultured in 6 well plates to a confluency of 60%. Cells were either cultured with 10% SS in D-MEM or cultured in the presence of inhibitors under serum starved conditions. Cells were lysed in culture dishes using TRIzol Reagent (Invitrogen, Carlsbad, CA) at 1 mL per 10 cm^2. Treated cells were kept on ice for 15 minutes. Cells were scraped, and transferred to sterile 1.5 mL microcentrifuge tubes. Chloroform was added, at 0.02 mL per 1 mL of TRIzol Reagent. The tubes were shaken vigorously and allowed to incubate for 20 minutes at room temperature. Samples were then centrifuged at 16,000 x g at 4°C for 20 minutes. Each supernatant was carefully removed avoiding protein contamination and placed into a new microcentrifuge tube. Then, 2-proponal was added, at 0.05 mL per 1 mL of TRIzol, inverted several times and the samples were incubated at 4°C for 15 minutes. The samples were then centrifuged at 16,000 x g at 4°C for 15 minutes. The supernatant was completely removed and the pellet was washed in 70% ethanol/RNase free water. The samples were again centrifuged at 16,000 x g at 4°C for 3 minutes. The supernatant was removed, and the pellet was air dried, allowing all of the ethanol to evaporate. The pellet was dissolved in RNase free water, in relation to pellet size. The concentration of RNA was measured using a Nano-drop Spectrophotometer ND-1000 (Nano Technologies, Wilmington, DE), with the blank being the RNase free water. The RNA samples were stored at -20°C for further use.

2.4 cDNA synthesis

The following steps were used to synthesize cDNA from each sample. A mixture of 2 μg of total RNA, 1 μL oligo$(dT)_{18}$ primer, 1 μL dNTPs (10 mM final concentration)

and adjusted to 20 μL by RNase free ddH_2O was prepared. The mixture was heat shocked at 70°C for 5 minutes then immediately put on ice for 1 minute. To the samples, 6 μL 5x reaction buffer (Invitrogen, Carlsbad, CA), 1 μL 0.01 M DTT, 0.5 μL RNase Inhibitor RNase OUT (Invitrogen, Carlsbad, CA), and 0.5 μL Superscript II (200 U/μL) (Invitrogen, Carlsbad, CA) was added. The samples were mixed by pipetting, and then allowed to incubate at 52°C for 1 hour for cDNA synthesis. The reaction was then stopped by heating at 72°C for 15 minutes. The synthesized cDNA was stored at -20°C for further use.

2.5 Quantitative Real Time Polymerase Chain Reaction

Quantitative Real Time PCR (qRT-PCR) was performed using MicroAmp Fast 96 well reaction plates (Applied Biosystems, Foster City, CA). A pre-made mixture of 5 μL of 2x SYBR qPCR Master Mix (Fermentas, Ukraine), 3 μL ddH_2O, and 1 μL 1/10 primer mix (Primers in Table 3), per well were made. 9 μL of the pre-made mixture and 1 μL of cDNA samples prepared from 2 μg of total RNA in 20μL, which were made as described above, were added to each well. An adhesive film (VWR, West Chester, PA) was placed over the reaction plate. The plate was centrifuged at 800 rpm at 4°C for 5 minutes. Each cDNA sample was prepared in triplicate. The housekeeping gene tubulin was used as a standard to compare background levels of cDNA. The reaction plate was run in 7500 Fast Real-Time PCR System (Applied Biosystems, Foster City, CA) using 7500 Fast System SDS Software for the further quantitative analysis which originally provided with the system.

Tubulin	
Sense	5’ AGAGGGCTTTGTGCTGTGTC 3’
Anti-sense	5’ ACCAGCTTCTTAGGATACCTGT 3’
CXCL5	
Sense	5’ GTGTTGAGAGAGCTGCGTTG 3’
Anti-sense	5’ CTATGGCGAACACTTGCAGA 3’
CXCL8	
Sense	5’ GTGCAGTTTTGCCAAGGAGT 3’
Anti-sense	5’ CTCTGCACCCAGTTTTCCTT 3’
VEGF-C	
Sense	5’ TCCTTTCCTTAGCTGACACTTGT 3’
Anti-Sense	5’ CACGGCTTATGCAAGCAAAGA 3’
$VEGF_{165}$	
Sense	5’ CAAGGCCCACAGGGATTTTC 3’
Anti-sense	5’ ATCTTCAAGCCATCCTGTGTGC 3’

Table 3. qRT-PCR Primer Sequences

2.6 Cell Lysates

Cell lysates were prepared as follows, with all steps being performed on ice. A cell lysis buffer solution of 10 mL 1 M HEPES pH 7.5, 10 mL 0.5 M EGTA pH 8.0, 4.32 g β-glycerolphosphate, 5 mL 1 M NP-40 lysis buffer, and 625 μL 2 M $MgCl_2$ per 500 mL was prepared. Lysis buffer solution was kept at 4°C. To this, 50 μL 1 M DTT, 500 μL 0.1 M PMSF, 50 μL 10 mg/mL aprotinin, 50 μL 10 mg/mL leupeptin, and 100 μL 1 M orthovanadate (184 mg/mL), per 50 mL of lysis buffer solution was added. Cells were cultured for 24 hours in an incubator at 37°C, with 90% air and 10% CO_2. Then culture medium was removed, and the cells were washed with cold PBS twice quickly, and then completely removed. The cell lysis solution was added in amount based on cell confluency and remained on ice for up to 20 minutes. Cells were then scraped from the bottom of the wells and transferred in sterile microcentrifuge tubes on ice. Samples were centrifuged at 16,000 x g for 15 minutes at 4°C. The supernatant was then removed, and placed in a sterile microcentrifuge tubes. The cell lysates were stored at -20°C for further applications.

2.7 Western Blotting

Protein concentration of cell lysates were measured by using BioRad Protein Assay Kit (BioRad Laboratories, Hercules, CA), which is based on the Bradford method, testing unknowns lysed protein samples against serially diluted 10 mg/mL bovine serum albumin (BSA). The protein concentration present in the lysates was calculated using a standard curve and samples were prepared by diluting with lysis buffer, to make the least concentrated sample, 20 μL. To each sample 4 μL of 6x SDS-PAGE loading buffer was

added before application to each well. The samples were heat shocked at 100°C for 5 minutes on the heat block then immediately placed on ice. The samples were spun-down and 16 μL of each sample was loaded into each well of the 10% SDS-PAGE gel. The gel was run for 1.5 hours at 120 V, 400 mA in 1x SDS-PAGE running buffer (20 mM Tris-Cl (pH 7.9), 100 mM NaCl, 70 mM EDTA, 2% SDS). Proteins were then transferred to Immobilon-P (Millipore, Bedford, MA) polyvinylidene difluoride membrane for at least 18 hours, at a constant 5 mA. The membrane was then blocked with 3% dried non-fat milk (Nestle, Glendale, CA) in 0.03% Tween-TBS (Tris-buffered saline) (T-TBS) for 1 hour on a shaker at room temperature. After blocking, the membrane was washed twice quickly, and 3 times with 5 minutes of rocking in between washes with T-TBS. The membrane was then incubated with 1:1000 (1 μg/mL) diluted antibodies, in 0.03% BSA in T-TBS or 0.03% milk in T-TBS, per manufactures instructions for overnight at 4°C. Antibodies used include; actin (I-19, Santa Cruz, SC1616 Lot #F0308, Anti-Goat), Anti-p38αMAPK (Cell Signaling, #2371 Lot 1, Anti-Rabbit), Anti-phospho-p38 MAPK (Thr180/Tyr182) (Cell Signaling, #9215S, Lot 4, Anti-Rabbit), Anti-Akt antibody (Cell Signaling, #9272, Lot 18, Anti-Rabbit), Anti-phospho-Akt (Ser473) (Cell Signaling, #9271S, Lot 11, Anti-Rabbit), Anti-p44/42 MAPK (Erk1/2) (Cell Signaling, #4695, Lot 5, Anti-Rabbit), Anti-phospho-p44/42 MAPK (Erk1/2) (Thr202/Tyr204) (Cell Signaling, #9106S, Lot 27, Anti-Mouse). After overnight incubation, the membrane was washed twice quickly, twice with 5 minutes rocking, and once with 10 minutes rocking at room temperature. Appropriate secondary antibodies were selected, and diluted 1:5000 (1 μl / 5 mL) in 0.03% non-fat dry milk in T-TBS, and rocked for 1 hour at room temperature. The membrane was washed twice quickly, twice with 5 minutes rocking, and twice with

10 minutes rocking at room temperature. Target protein was then detected using Western Lightning Chemiluminescence Plus system (Perkin-Elmer, Shelton, CT) following manufactures instructions. Membranes were developed using a Kodak photo-processor, with Blue Devil autoradiography film (Genesee Scientific, San Diego, CA).

2.8 Plasmid Preparation

The pSirenRetroQ plasmid vector (Clontech, Mountain View, CA) was digested with appropriate restriction enzymes. This was done by addition of 20 U/μL of each enzyme, 10x BSA, 10x NEBuffer #2 (New England Biolabs, Ipswich, MA), 200 ng pSirenRetroQ plasmid and 6 μL ddH_2O. The sample was incubated in a 37°C water bath for a least 1 hour. To subclone the insert to the plasmid, in a sterilized microcentrifuge tube, 100 ng insert, 100 ng plasmid, 4 μL of 5x T4 DNA ligase Buffer (250 mM Tris-HCl pH 7.6, 50 mM $MgCl_2$, 5 mM ATP, 5 mM DTT and 25% (w/v) polyethylene glycol-8000), ddH_2O to 19.5 μL and 0.5 μL T4 DNA ligase (Invitrogen, Carlsbad, CA) were added. The solution was incubated at room temperature for 2 hours. The digested contents were run on a 1% agarose gel. The gel was run at 120 V, 400 mA for 15 to 30 minutes with 3 μL HyperLadder II DNA marker (Bioline, Tauton, MA). After the enzyme digested samples were run on the gel, the appropriate bands were purified using QIAEX II Gel Extraction Kit (Qiagen, Valencia, CA) following manufacture's protocol. The band was excised from the gel using a clean, sharp scalpel and placed into a 1.5 mL microcentrifuge tube. The sample was weighed, and 300 μL of buffer QX1 to each 100 mg of gel and incubated until gel completely dissolved. Then QXII was resuspended by vortexing at room temperature for one minute. 10 μL of QXII was added per 2 μg of

DNA. The sample was incubated at 50°C for 10 minutes to bind the silica-based beads to the solution suspended DNA. The sample was mixed every 2 minutes by vortexing for 2 minutes. The sample was centrifuged at 16,000 x g at room temperature for 30 seconds and the supernatant was discarded. The pellet was washed with 500 μL of buffer QX1. Then the pellet was washed twice with 500 μL of washing buffer PE. The pellet was air-dried for 10 to 15 minutes. 20 μL of DNase free ddH_2O was used to resuspend the pellet and vortexed. The sample was then centrifuged at 16,000 x g at room temperature for 30 seconds. The DNA eluted supernatant was removed and placed into a clean microcentrifuge tube. The concentration of DNA was measured using a Nano-drop Spectrophotometer (ND-1000, Nano Technologies, Wilmington, DE). Eluted DNA samples were stocked at -20°C for further enzymatic modification.

2.9 *E. coli* Transformation

E. coli cells were stored at -80°C and were thawed on ice. 2 μg of DNA was added to 50 μL of competent *E. coli* cells, and mixed by gentle swirling. The cells were then incubated on ice for 30 minutes, placed in a 42°C water bath for 30 seconds, and then immediately back on ice for 3 minutes. Then 500 μL of warmed SOC medium (2% tryptone, 0.5% yeast extract, 0.4% glucose, 10 mM NaCl, 2.5 mM KCl, 10 mM $MgCl_2$, and 10 mM $MgSO_4$) was added to each sample. The tubes were then placed in a 37°C air incubator and shook at 200 rpm for 60 minutes. The cells were then plated on LB (Luria-Bertani) agar plates containing 50 μg/mL ampicillin and incubated overnight at 37°C. Colonies were then picked up and inoculated in 50 μg/mL ampicillin containing LB broth, and allowed to culture overnight.

2.10 DNA Purification System

DNA was purified from overnight cultured competent *E. coli* cells using Wizard Plus SV Minipreps DNA Purification System (Promega Madison, WI). 1.5 mL of overnight ampicillin containing LB broth was pelleted for at 16,000 x g at room temperature for 1 minute. The supernatant was discarded and the pellet was resuspended in 250 μL of resuspension cell solution. Then 250 μL of cell lysis solution was added to the sample, and it was inverted 4 times. 10 μL of alkaline protease solution was added to the sample, and then inverted 4 times. The sample was allowed to incubate at room temperature for 5 minutes. 350 μL of neutralization solution was then added to the sample, and inverted 4 times. The sample was centrifuged at 16,000 x g at room temperature for 10 minutes. The clear lysate was transferred to a spin column, which had been inserted into a collection tube. The spin column and collection tube were spun at 16,000 x g at room temperature for 1 minute. 750 μL of washing solution was added to the column, and spun at 16,000 x g at room temperature for 1 minute. The flow through was discarded, and then the column was rewashed with 250 μL washing solution and additionally spun for 2 minutes at 16,000 x g at room temperature. The spin column was transferred to a new sterile 1.5 mL microcentrifuge tube. 100 μL of DNase free clean water was added to the spin column and spun at 16,000 x g at room temperature for 1 minute. Collected DNA concentration and purity was measured using the Nano-drop Spectrophotometer. The processed DNA was stored at -20°C for further use.

2.11 Cell Transfection

HN4 or HN12 cells were grown to 60% confluency. 400 μL of serum free medium, 2 μL of Turbofect (Fermentas, Glen Burnie, MD), and 1 μg of DNA per 10 cm plate was mixed in a 1.5 mL eppendorf tube and incubated for 15 minutes. While incubating, cell culture medium was replaced with fresh medium contain 10% Serum Supreme (Lonza, Walkersville, MD). After the 15-minute incubation period, the DNA and Turbofect contained mixture was added dropwise to the cell culture plates. The plates were then rocked briefly to evenly distribute the solution across the bottom of the plate. Plates were then immediately returned to air incubator at 37°C, and 90% air and 10% CO_2. Transformed colonies were selected by treatment with D-MEM containing puromycin.

2.12 Dual Luciferase Reporter Assay System

Dual Luciferase Reporter (DLR) assay system manufactured by Promega (Madison, WI) was used to determine level of gene transcription. In the DLR assay, the activity of firefly (*Photinus pyralis*) and *Renilla* (*Renilla reniformis* or sea pansy) luciferases are measured sequentially from the same sample. HN4 and HN12 cells were cultured in 24 well plates with 10% Serum Supreme in D-MEM to a confluency of at least 70%, as followed by manufacturer's protocol. Cells were washed with PBS, and all liquid was aspirated off. A 1X Passive Lysis Buffer (PLB) was prepared and 50 μL was dispensed into each well. Cells were lysed at room temperature for 15 minutes. Luciferase Assay Reagent II (LAR II) was aliquoted, 100 μL, into eppendorf tubes. While the cells were lysing, Stop and Glo Substrate was prepared to a 1X final

concentration. After 15 minutes passed, the cells were collected by scraping the bottom of each well and 20 μL of cell lysate was suspended into LARII, and mixed well. Firefly luminescent is measured using a luminometer (Turner BioSystems, Sunnyvale, CA). After quantifying the firefly luminescence, the reaction is quenched, and the *Renilla* luciferase reaction is initiated simultaneously by adding 100 μL Stop of Glo Reagent.

Results

3.1 HN4 and HN12 Expression

In order to study the biological mechanisms of HNSCC, we used two cell lines derived from one male patient. These cell lines are designated HN4 and HN12. The HN4 cell line was established from a primary squamous cell carcinoma of the tongue and the HN12 cell line from a lymph node metastasis. Since these cell lines were derived from one patient, it minimizes the background genetic variation. This makes this a comparison based model system more reliable, which is rarely available in head and neck cancer research. A previous study with this pair of cell lines using a cDNA microarray showed that the expression levels of CXCL5 and CXCL8 were upregulated in the HN12 cell line, 7.3 and 2.2 times respectively, versus the HN4 cell line (Miyazaki 2007). Before we start this research, we performed qRT-PCR to compare the expression status of CXCL5, CXCL8, VEGF-C and $VEGF_{165}$ currently in our cell lines. Current work with these cell lines showed the higher expression of CXCL5, 4.5 times (Figure 6a), but no longer the higher expression of CXCL8, as CXCL8 expression in HN12 was almost to levels of HN4, which expresses minimally low detectable levels of CXCL8 (Figure 6b). We recovered previously used and stocked original cell lines and tried to recover the same molecular expression profiles but CXCL8 expression status was unrecoverable. The overexpression of VEGF-C, the predominant VEGF involved in lymphangiogenesis, has also been observed more highly expressed, 3 times, in HN12, versus HN4 cell line (Figure 6c). The expression of $VEGF_{165}$, the dominantly expressed VEGF-A isoform, which has been shown to be involved in angiogenesis was also studied. In our current cell lines we did not see a difference in expression of $VEGF_{165}$ between HN4 and HN12

(Figure 6c). The significant higher expression of CXCL5 and VEGF-C in HN12 are the essential differences between these cell lines which will be examined.

a.

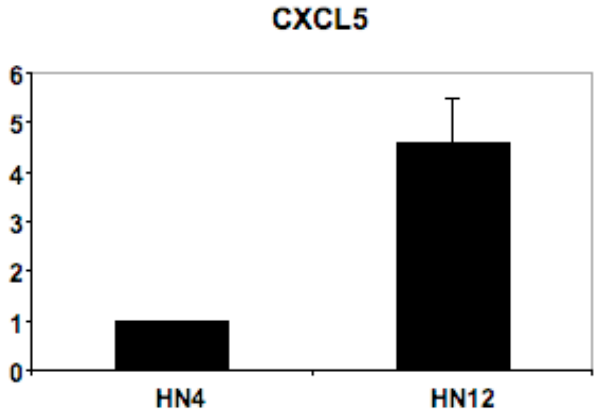
CXCL5
6
5
4
3
2
1
0
HN4
HN12

b.

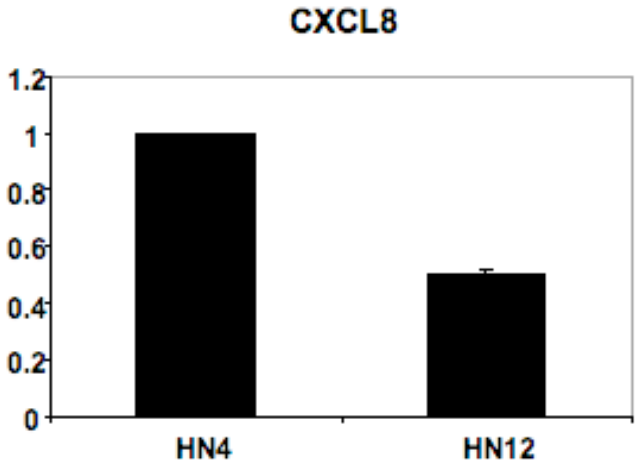
CXCL8
1.2
1
0.8
0.6
0.4
0.2
0
HN4
HN12

c.

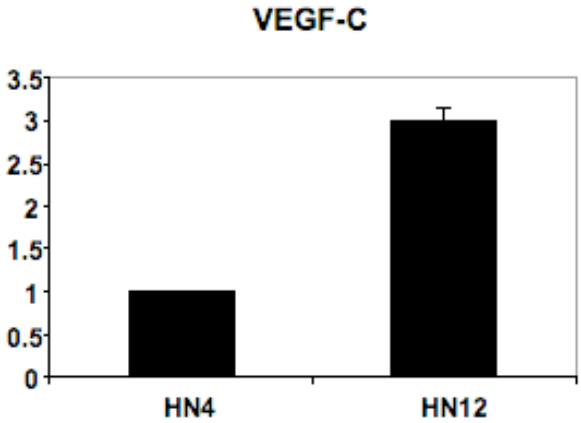
VEGF-C
3.5
3
2.5
2
1.5
1
0.5
0
HN4
HN12

d.

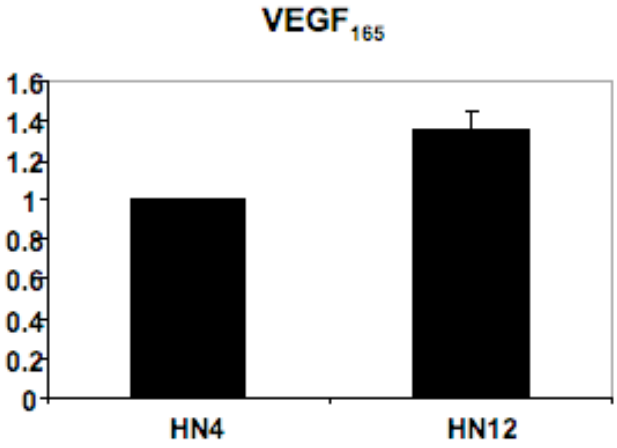

Figure 6. Total RNA was extracted from HN4 and HN12 cell lines cultured in 10%SS containing D-MEM, reverse transcribed, and qRT-PCR was performed as described in materials and methods. Values were standardized to the housekeeping gene tubulin. Assays were performed in triplicate with a standard deviation of < .1. These graphs show the relative expression of (a) CXCL5, (b) CXCL8, (c) VEGF-C and (d) $VEGF_{165}$ present in HN4 and HN12 cell lines.

3.2 Cell Proliferation

HN4 and HN12 cell lines have been shown to grow at different proliferation rates. The primary cell line HN4 grows at a slower rate relative to HN12, and in a more linear fashion. The metastatic cell line HN12 has a faster proliferation rate and displays an exponential proliferation curve. The different proliferation rate of HN4 and HN12 cell lines can be seen in figure 7. HN4 and HN12 cell numbers were originally matched and cultured in 24-well plates with 10% SS containing D-MEM in incubator at 37°C, with 90% air and 10% CO_2. Four wells were trypsinized daily as described in materials and methods and counted up to 9 days. Each well was individually counted using the hemocytometer and then average and standard deviation was calculated. During the first 6 days HN4 and HN12 cells did not show a difference in the cell number until after day 6, when HN12 grew at an increased exponential rate (Figure 7). From day 7 through day 9, we can see the exponential proliferation rate of the HN12 versus HN4. By day 9, HN12 averaged 3 times as many cells as HN4. After day 9, the cells become completely confluent and begin to reach a plateau. We terminated the proliferation assay after we confirmed it. This assay was repeated 3 times and averaged as described.

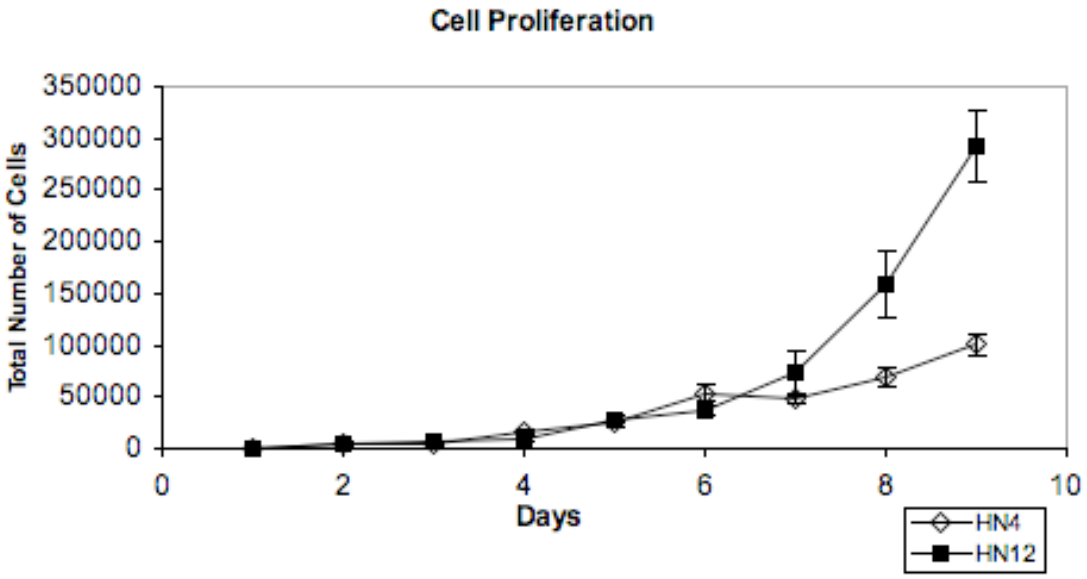

Figure 7. The graph shows the proliferation of HN4 and HN12 cell lines when cultured in 10% SS containing D-MEM. Cell numbers were matched and then four individual wells were trypsinized and counted as described in materials and methods daily for 9 days. Experiments were performed 3 times and averaged, and then the standard deviation was added.

3.3 Cell Proliferation in the Presence of Inhibitors

In order to study the kinase pathways involved in chemokines and VEGFs expression, we dissected the role of the Akt/PI3-K, MAPK Erk 1/2 and p38 MAP kinase pathways in our cell lines HN4 and HN12. In order to examine each one of these pathways individually, inhibitors of each of these pathways were added independently to these cell lines and expression changes were analyzed using qRT-PCR. In order to determine the impact these inhibitors could have on these cell lines, HN4 and HN12 cells were cultured in the presence of Akt inhibitor LY294002 or MAPK inhibitor PD098059 and DMSO was used as a control, with 10% SS containing D-MEM in 24-wells plates. This proliferation assay was used to determine if the presence of inhibitors at final concentrations determined to knockdown these individual pathways would alter their proliferation rate. The presence of Akt inhibitor, LY294002, or MAPK inhibitor, PD098059, both at a final concentration of 10 μM did not affect the proliferation rate of HN4 or HN12 cell lines (Figure 8). In these assays, as well, HN12 cell lines proliferated about 5 times faster than HN4, similar to when these cell lines were cultured in the absence of inhibitors or with DMSO. The addition of inhibitors on these cell lines at a concentration to effectively knockdown the MAPK or Akt pathways did not show any effect on the rate of proliferation of the HN4 or HN12 cell line. This proliferation assay showed us that using these inhibitors, at the tested concentrations, on these cell lines will not affect their proliferation rate.

a.

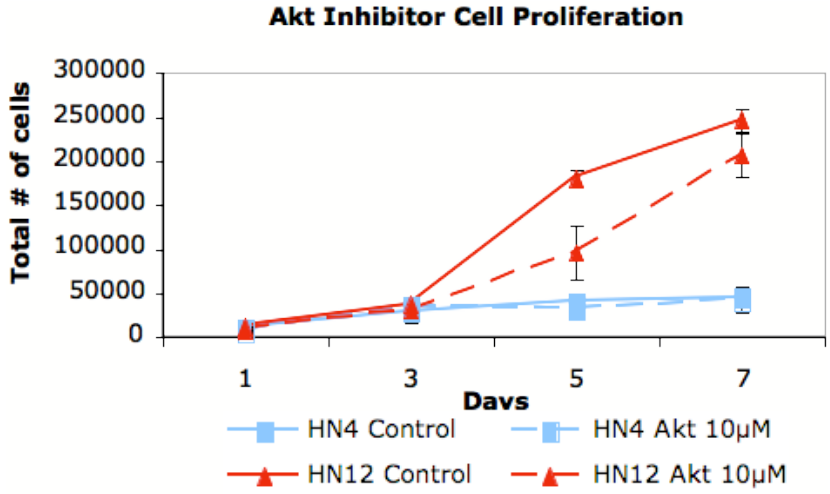

b.

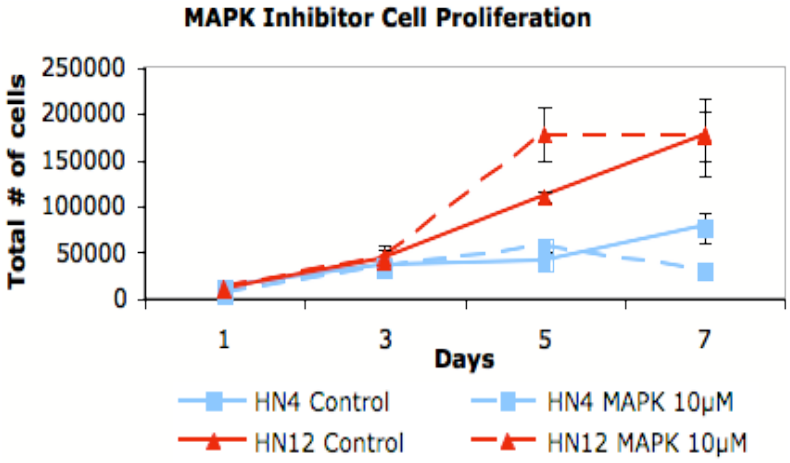

Figure 8. These graphs show the cell proliferation rate of HN4 and HN12 cells cultured in 10% SS containing D-MEM in 24-wells plates with the presence of Akt inhibitor, LY294002, (a) or MAPK inhibitor, PD098059, (b) at a final concentration of 10 μM and DMSO was used for the control. Four individual wells were counted every other day as described in materials and methods, averaged and the standard deviation was added.

3.4 Pathway Inhibition

Recently several groups published works that PI3-K/Akt (Raman 2007, Tsai 2003), p38 MAP kinase (Trevino 2005, Tsai 2003), and p44/42 MAPK pathways (Trevino 2005, Tsai 2003) are essential for chemokine expression as well as VEGFs expression. In order to study the role and contributions of each of these individual pathways, each were individually inhibited using commercially available inhibitors (see materials and methods). The cell lines, HN4 and HN12, have been used for many years in our laboratory and we wanted to reconfirm its kinase activity before we started these kinase inhibition studies in normal cell culture conditions. We performed preliminary western blot analysis and confirmed that in general, all 3 kinase pathways are activated in HN12 cell line. After we confirmed this fact, we applied inhibitors to examine the subsequent effects of downregulation each kinase on the expression status of chemokines, CXCL5 and CXCL8, as well as VEGF-C and $VEGF_{165}$. First, the appropriate final concentration of inhibitor necessary to knockdown each of these individual pathways in HN4 and HN12 cell lines was determined based on several criteria. First, the inhibitor needed to effectively knockdown the signaling pathway. Second, it should not be biologically hazardous to the cell lines. Third, it must be shown to not affect other kinase pathways. Cells were cultured in 6 well plates for 24 hours in 10% SS containing D-MEM. Serum containing medium was removed after 24 hours and the cells were washed with PBS. Cell medium were then replaced with serum free medium containing the indicated inhibitors and cultured for 18 hours. After 24 hours of serum starvation, the knockdown of each pathway was observed by performing western blot analysis as described in material and methods. The amount of inhibition was determined by using

Image J software (NIH). The integrated densities of bands present on the western blots were determined by digitally subtracting the background noise. The inhibited integrated density was then standardized by the control to calculate the relative inhibition obtained with each inhibitor. Experiments were done in triplicate and averaged and the standard deviation was calculated for each averaged output. Even concentration was determined by checking expression of Akt, p38, MAPK and actin by western blot using same membrane, which was used for the measurement of phosphorylation of each kinase.

3.5 Akt Inhibitor LY294002

The cell lines, HN4 and HN12, were cultured as described above in the presence of pharmacological Akt inhibitor, LY294002. The cells were then lysed, or RNA extracted and cDNA synthesized, and qRT-PCR was performed as described in the materials and methods. The levels of tubulin, CXCL5, CXCL8, VEGF-C and $VEGF_{165}$ were calculated. The expressions of chemokines or VEGF-C were determined by comparison to serial dilutions ranging from 10^{-5} to 10^{-8}. Expression level of tubulin, a housekeeping gene, was determined in each cDNA sample, and used to standardize the amount of each cDNA sample. The expression of chemokine or growth factor in the presence of inhibitor was then compared, by standardizing the control to a value of 1. Each trial was prepared in triplicate per plate and then averaged with a standard deviation of < .01. Multiple trial data were then averaged and the standard deviation was added.

Akt inhibitor, LY294002, was tested at a final concentration of 5 μM and 10 μM (Figure 9a). 10 μM was determined to be an effective concentration to decrease Akt phosphorylation in both HN4 and HN12. The Akt activity in HN4 cell line was reduced

to 20%, where as in HN12 cell line it was reduced to 50%, (Figure 9b) of original activation without addition of the inhibitor.

After the effective final concentration of inhibitor was determined, qRT-PCR was performed to determine the levels of chemokines and VEGFs expression. qRT-PCR data showed a 60% downregulation of CXCL5 transcription in HN4, and negligible reduction in HN12 (Figure 10a) with inhibition of Akt. CXCL8 was determined to be downregulated 40% in both HN4 and HN12 (Figure 10b). Inhibition of the Akt pathway did not clearly affect the expression of VEGF-C in HN4, but showed a 100% upregulation in HN12 (Figure 10c). $VEGF_{165}$ expression was upregulated 3 times in HN4 with the inhibition of the Akt pathway. In the HN12 cell line, inhibiting the Akt pathway caused a 50% downregulation in the expression of $VEGF_{165}$. The expression of chemokines, CXCL5 and CXCL8, were both downregulated in HN12, less significantly in CXCL5, with the inhibition of the Akt pathway. The VEGF-C expression was however upregulated in HN12 with the inhibition of Akt, but $VEGF_{165}$ was downregulated in this cell line.

a.

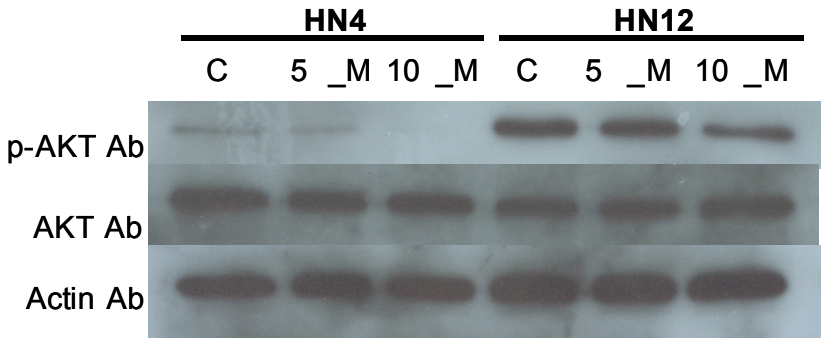

b.

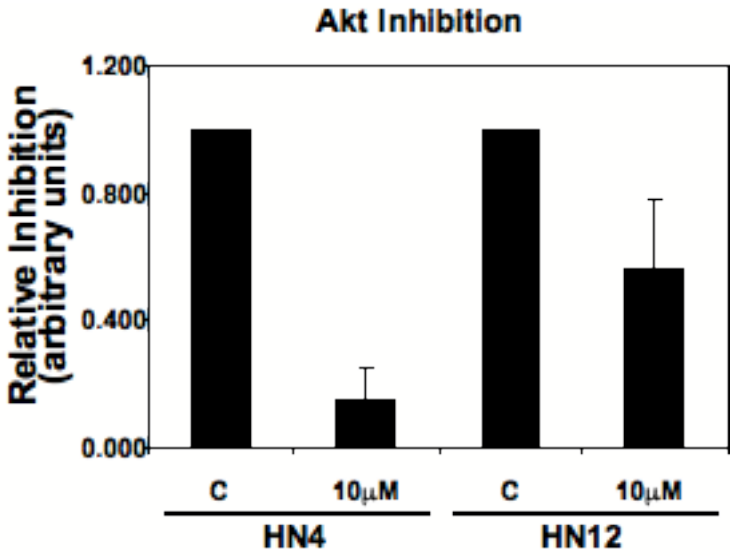

Figure 9. HN4 and HN12 cells were cultured using serum free medium with DMSO as a control and Akt inhibitor (LY294002) at various concentrations and the western blot (a) is shown. The membrane was incubated with phospo-Akt antibody overnight. Even concentration was determined by Akt antibody and actin antibody. The films were scanned and Image J was used to determine the relative density and intensity of the bands. (b) The integrated density was graphed, standardizing the control (DMSO) equal to 1, to show the relative inhibition with addition of Akt inhibitor (LY294002) to cell culture.

a.

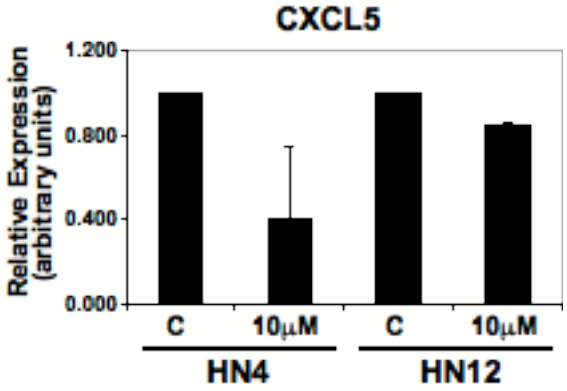
CXCL5
Relative Expression (arbitrary units)
1.200
0.800
0.400
0.000
C
10μM
C
10μM
HN4
HN12

b.

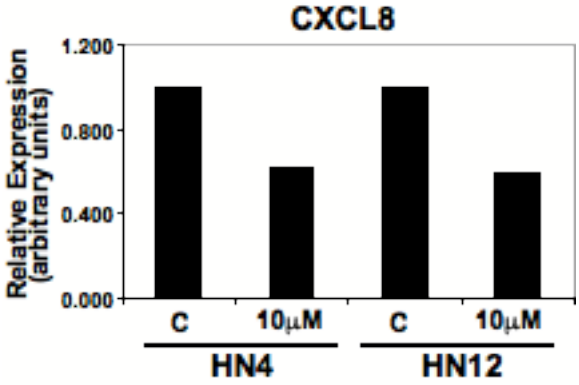
CXCL8
Relative Expression (arbitrary units)
1.200
0.800
0.400
0.000
C
10μM
C
10μM
HN4
HN12

c.

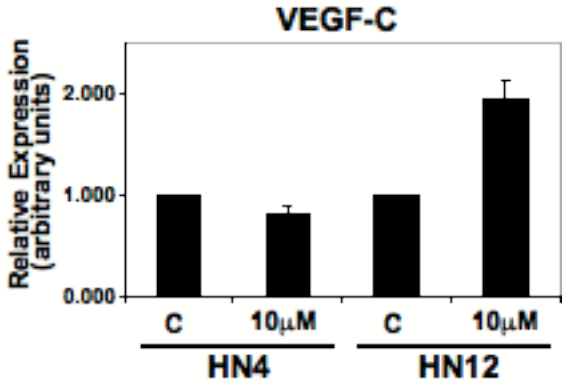
VEGF-C
Relative Expression (arbitrary units)
2.000
1.000
0.000
C
10μM
C
10μM
HN4
HN12

d.

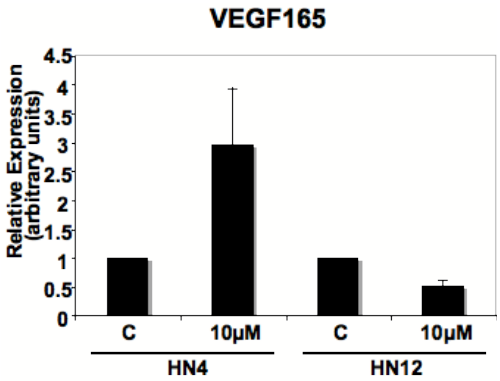

Figure 10. qRT-PCR was performed as described in materials and methods. These graphs show the relative expression of (a) CXCL5, (b) CXCL8, (c) VEGF-C and (d) $VEGF_{165}$ present in HN4 and HN12 cells cultured with Akt inhibitor (LY294002) at a final concentration of 10 μM.

3.6 MAPK Inhibitor PD098059

The cell lines, HN4 and HN12, were cultured in the presence of MAPK inhibitor PD098059. The cells were then lysed, or RNA extracted and cDNA synthesized, and qRT-PCR was performed as described in the materials and methods. The levels of tubulin, CXCL5, CXCL8, VEGF-C and $VEGF_{165}$ were calculated. The expression levels of chemokines or VEGFs were determined by comparison to standard serially diluted samples from 10^{-5} to 10^{-8}. Levels of tubulin were determined in each cDNA sample, and used to standardize the amount of each cDNA. The expression levels of chemokines or VEGFs were then compared, by standardizing the control to a value of 1. Each trial was prepared in triplicate per plate and averaged with a standard deviation of < .01. Multiple trials were performed to obtain stable data.

MAPK inhibitor PD098059 was tested at final concentrations 5 μM and 10 μM (Figure 11a). 10 μM was determined to be an effective final concentration to inhibit MAPK in both cell lines HN4 and HN12. The phosphorylation level of MAPK pathway in HN4 cell line was reduced to 20%, where as in HN12 cell line it was reduced to 10% as compared to the control phosphorylation level (Figure 11b).

qRT-PCR data showed an upregulation of 50% of CXCL5 in HN4 and HN12 (Figure 12a) in the presence of 10μM MAPK inhibitor. Another proangiogenic chemokine CXCL8 exhibited 180% upregulated in HN12, but only 20% upregulation was observed in HN4 (Figure 12b) with application of this inhibitor. Inhibition of the MAPK pathway did not seem to affect the expression level of VEGF-C in HN4, but 100% upregulation in HN12 was observed (Figure 12c). Expression of $VEGF_{165}$ was downregulated 80% in both HN4 and HN12 with the inhibition of the MAPK pathway

(Figure 10d). The expression level of proangiogenic chemokines, CXCL5 and CXCL8, were both upregulated with the inhibition of the MAPK pathway. The VEGF-C expression level as well was significantly upregulated 100% in HN12, but there was an 80% downregulation in levels of $VEGF_{165}$ in HN4 and HN12 with the inhibition of MAPK.

a.

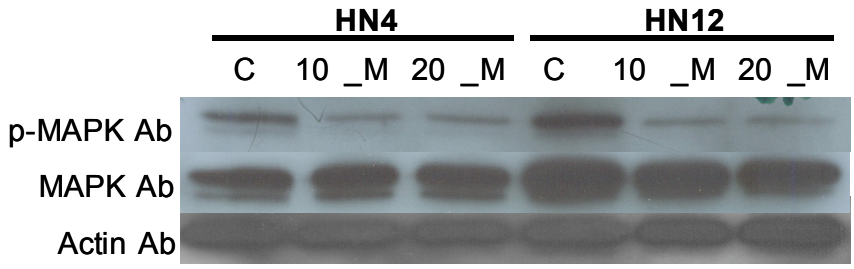

b.

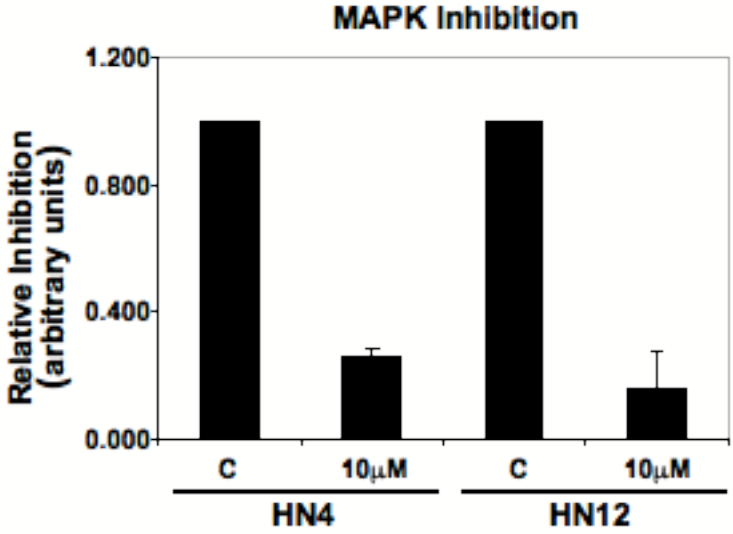

Figure 11. HN4 and HN12 cells were cultured using serum free medium with DMSO as a control and MAPK inhibitor (PD098059) at various concentrations and the western blot (a) is shown. The membrane was incubated overnight with phospo-MAPK antibody. Even concentration was confirmed by MAPK antibody and actin antibody. The films were scanned and Image J was used to determine the relative density and intensity of the bands. (b) The integrated density was graphed, standardizing the control (DMSO) equal to 1, to show the relative inhibition with addition of Akt inhibitor (LY294002) to cell culture.

a.

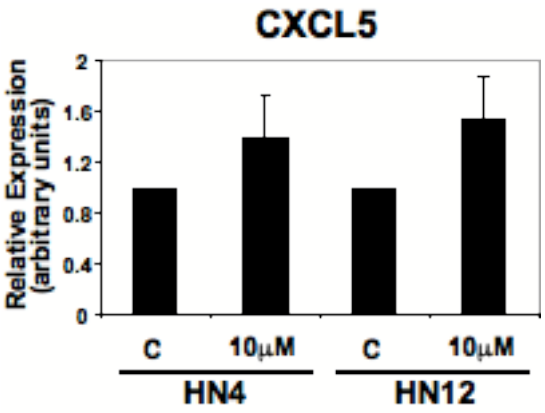
CXCL5
Relative Expression (arbitrary units)
2
1.6
1.2
0.8
0.4
0
C
10μM
C
10μM
HN4
HN12

b.

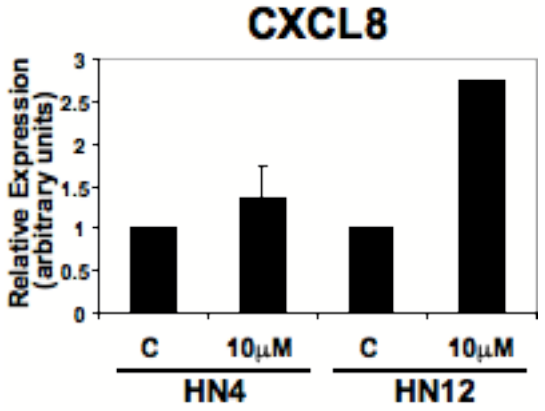
CXCL8
Relative Expression (arbitrary units)
3
2.5
2
1.5
1
0.5
0
C
10μM
C
10μM
HN4
HN12

c.

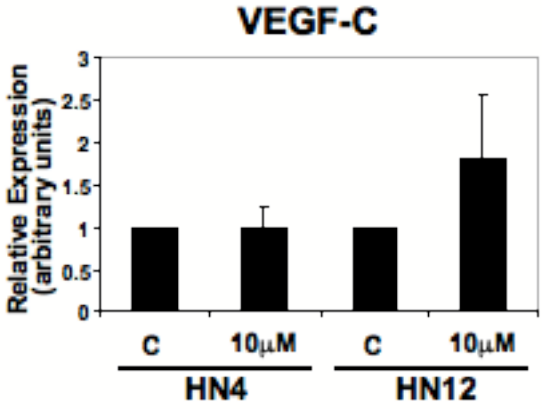
VEGF-C
Relative Expression (arbitrary units)
3
2.5
2
1.5
1
0.5
0
C
10μM
C
10μM
HN4
HN12

d.

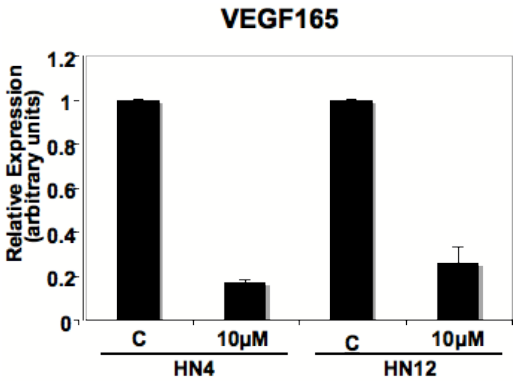

Figure 12. qRT-PCR was performed as described in materials and methods. These graphs show the relative expression of (a) CXCL5, (b) CXCL8, (c) VEGF-C, and (d) $VEGF_{165}$ present in HN4 and HN12 cells cultured with MAPK inhibitor (PD098059) at a final concentration of 10 μM.

3.7 p38 MAP Kinase Inhibitor SB203580

p38 MAP kinase inhibitor SB203580 was tested at a final concentration of 5 μM, 10 μM (Figure 13a), 25 μM, 50 μM (Figure 13b) and 100 μM (Figure 13c). None of these concentrations showed effective to decrease the activated p38 MAP kinase pathway. On the contrary, the western blot analysis with these concentrations exhibited activation of p38 MAP kinase instead of downregulation in both HN4 and HN12. This inhibitor was not effective as a p38 MAP kinase inhibitor in our cell lines, and this p38 MAP kinase inhibitor was replaced with a freshly purchased sample to avoid possible degradation or penetration of inhibitor.

a.

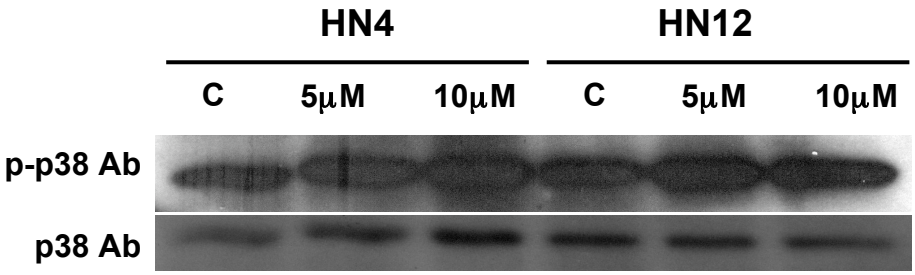

b.

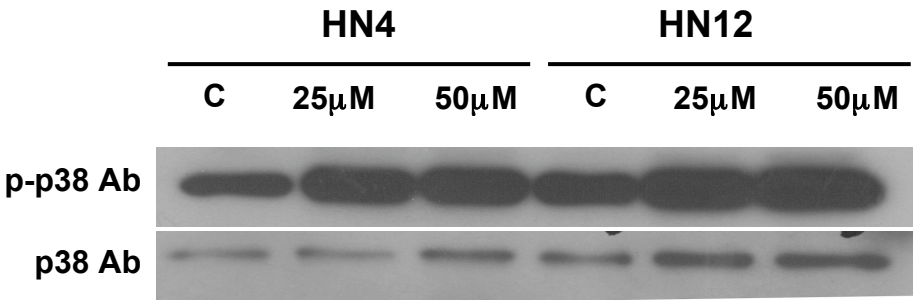

c.

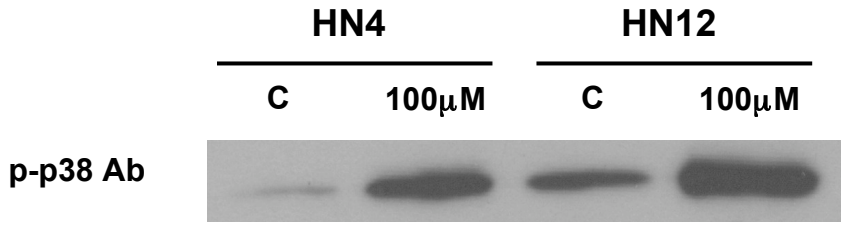

Figure 13. HN4 and HN12 cells were cultured in 6-well plates using serum free medium with DMSO as a control and p38 MAP kinase inhibitor (SB203580) at a final concentration of 5 μM, 10 μM (a), 25 μM, 50 μM (b) and 100 μM (c) for 24 hours. Western blots were performed as described in materials and methods. Membranes were incubated with phospho-p38, and even concentration was determined by αp38 MAP kinase antibody.

3.8 p38 MAP Kinase inhibitor SB202190

p38 MAP kinase inhibitor SB202190 was prepared to determine if it was capable of knocking down the activated p38 MAP kinase in our cell lines, HN4 and HN12. This inhibitor was tested at final concentrations of 25 μM and 50μM (Figure 14a). At these concentrations the activation of the p38 MAP kinase pathway was also not downregulated. The p38 MAP kinase inhibitor was then tested at a final concentration of 20 μM on the HN12 cell line at different time lengths of inhibition in serum starved conditions from 1 hour to 48 hours (Figure 14b). The p38 pathway seemed to be most activated at 4 hours with the presence of this inhibitor, and then returned to control levels after 48 hours. Combination of various time periods of exposure to inhibitor and serum starvation to the cells did not effectively downregulate the p38 MAP kinase pathway activation. The next approach to determine conditions that could effectively knockdown p38 MAP kinase was to culture the cells with the p38 MAP kinase inhibitor in the presence of serum, instead of serum free conditions to see the relative downregulation of p38 at final concentrations of 25 μM and 50 μM (Figure 14c). In these conditions based on western blot analysis, we still did not see a decrease in p38 MAP kinase phosphorylation versus DMSO applied control conditions.

a.

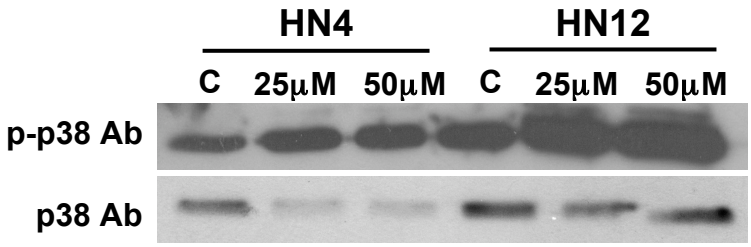

b.

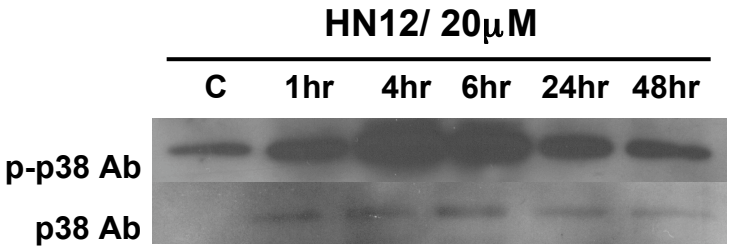

c.

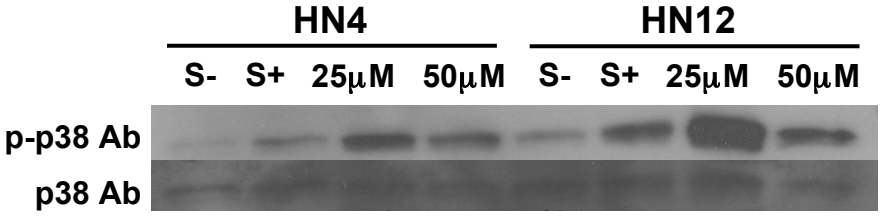

Figure 14. (a) HN4 and HN12 cells were cultured using serum free medium with DMSO as a control and p38 MAP kinase inhibitor (SB202190) at indicated final concentrations and the western blots are shown above. (b) The p38 MAP kinase inhibition experiment was also performed on HN12 cells with 20 μM SB202190, at different time periods of serum starvation. (c) SB202190 was also tested in the presence of serum, as well as serum free in the final concentration of 25 μM and 50 μM. The membranes were incubated with αphospo-p38 antibody overnight. Even concentration was confirmed by applying αp38 antibody antibody.

3.9 CXCR2 Inhibition

CXCR2 inhibitor, SB225002, was applied on HN4 and HN12 cell lines. This CXCR2 inhibitor competitively inhibits CXCL8 or CXCL5 by binding to CXCR2. This inhibitor was tested at the final concentrations of 10 μM and 20 μM, with serum starved conditions for 24 hours in 6-well plates. After 24 hours, RNA was extracted and cDNA was synthesized for qRT-PCR as described in materials and methods. Expression of VEGF-C and $VEGF_{165}$ was quantified by comparison to serially diluted standards from 10^{-5} to 10^{-8}. Levels of tubulin were also determined in each cDNA sample, and used to standardize the amount of each cDNA. The expression levels of VEGFs were then compared, by standardizing the control to a value of 1. Each trial was prepared in triplicate and then averaged with a standard deviation of < .01. Multiple trials were performed and then averaged and the standard deviation was calculated.

In the presence of CXCR2 inhibitor at final concentrations 10 μM and 20 μM expression levels of VEGF-C decreased 80% in HN4. In the HN12 cell line, however, expression levels of VEGF-C increased 50%, and 250%, with CXCR2 inhibitor, at 10 μM and 20 μM, respectively (Figure 15a). Expression levels of $VEGF_{165}$ decreased with the presences of CXCR2 inhibitor in both HN4 and HN12 cell lines. HN4 had a 40% decrease in $VEGF_{165}$ expression, and HN12 showed a 20% downregulation (Figure 15b). The inhibition of CXCL5 and CXCL8 receptor caused a downregulation in HN4 in expression of VEGF-C as well as $VEGF_{165}$. Inhibiting these chemokines signaling in HN12, caused an upregulation in VEGF-C, but a downregulation in $VEGF_{165}$.

a.

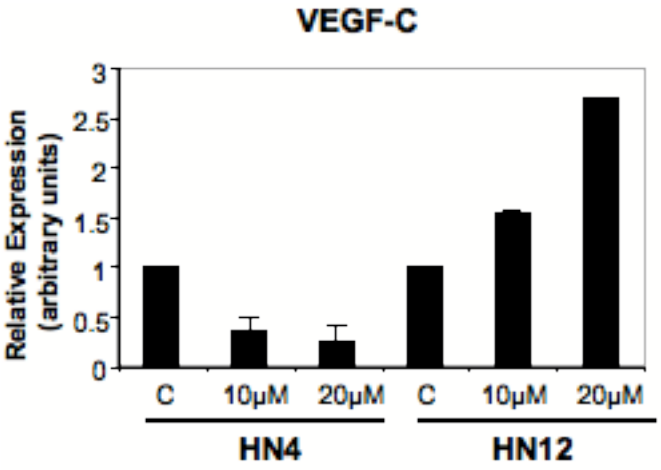

b.

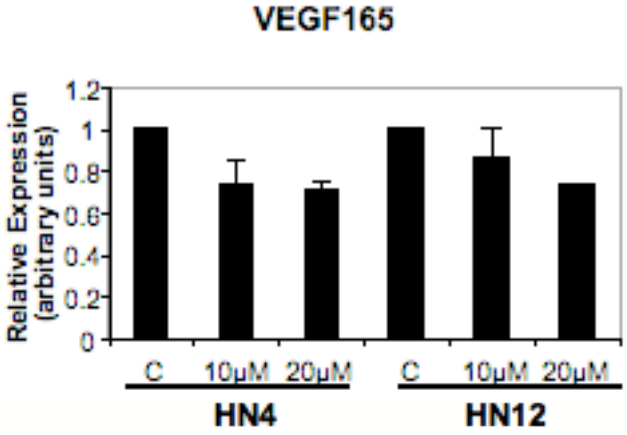

Figure 15. qRT-PCR was performed as described in materials and methods. These graphs show the relative expression levels of (a) VEGF-C (b) $VEGF_{165}$ present in HN4 and HN12 cells cultured with CXCR2 inhibitor SB225002 at a final concentration of 10 μM and 20 μM.

Discussion

4.1 Current Study

The aim of this study was to determine the roles of kinase activity on the expression levels of chemokines, CXCL5 and CXCL8, and VEGFs, A and C, in HNSCC. Previous reports showed that activation of the kinase pathways, such as Akt, MAPK, and p38 MAP kinase regulates the expression of these chemokines and VEGFs. The contributions of each of these pathways were further dissected to sort out how they regulate transcription of chemokines and VEGFs. Several different reports suggest the upregulation of these kinase activities are directly or indirectly inducing chemokine and/or VEGF expressions.

4.2 HNSCC Model System

In order to study the roles of these chemokines and VEGFs, we used an *in vitro* approach. Two HNSCC cell lines obtained from one patient have been isolated in different time periods and maintained in culture. The HN4 cell line was generated from a primary tumor of the tongue. The second cell line HN12 was derived from a lymph node metastasis in the same patient. Previously, our group performed a cDNA microarray analysis to analyze the molecular expression pattern between these two cell lines. These cell lines were established from one patient making the original genetic background minimal. Thus, comparing these two cell lines gives us a chance to compare the change of molecular expression data, which are acquired due to the development of the metastatic character. Through the cDNA microarray, we found approximately 60 genes were upregulated or downregulated between these two cell lines (Miyazaki 2006).

Among these, two chemokine genes, CXCL5 and CXCL8, were shown to be significantly upregulated in the HN12 cell line compared to its primary cell line HN4. These two chemokines will be further studied to investigate their role in metastasis.

Recently, these two chemokines have been shown to increase the metastatic ability of cells by our group. Another significant difference between HN4 and HN12 was the expression levels of VEGFs, especially VEGF-C. VEGF-C as well increases the cell's ability to metastasis, by their innate ability to induce lymphangiogenesis. Upon further investigation of these upregulated genes, CXC chemokines and VEGFs, it was shown that both of these groups activate similar kinase pathways. Therefore, we presumed that ELR(+) CXC chemokines CXCL5 and/or CXCL8 via binding to their receptor CXCR2, could induce or interfere with VEGF transcription by activating these MAP kinase pathways. We hypothesize possible mechanisms for this increased transcription as follows. The overexpression of CXCL5 and/or CXCL8 could induce upregulation of VEGF signaling pathways through a gene transcriptional upregulation of VEGFs. Another possibility is the activation of the kinase pathways, due to the overexpressed chemokines, may induce angiogenesis by interacting with VEGF's signaling pathways. These two hypotheses are not mutually exclusive, as it could also be a combination of these two phenomenons.

Multiple approaches were taken to determine the regulation of these chemokines and VEGFs. Inhibitors of each contributing kinase pathway were used to treat these cell lines. Western blot analysis and qRT-PCR were used to determine the impact of these inhibitors on these cell lines. The CXCL5 and CXCL8 receptor, CXCR2, was also inhibited, using a competitive pharmacological inhibitor, and qRT-PCR was used to

determine its impact on the VEGFs. As we already stated in the results part, we found that the CXCL8 expression level was not highly expressed in this freshly prepared HN12 cell line. It made it possible to compare the activity of these kinase activities after the application of this CXCR2 inhibitor. CXCL8 cannot induce downstream signaling activation because of its weak expression level. Therefore we can exclusively focus on the possible signaling activation through the highly upregulated CXCL5 and the application of CXCR2 inhibitor can tell the direct effect on downstream kinase activity through this chemokine. Results from these experiments will help to determine if there is a connection and what kind of signal activation dependency is present between the overexpression of chemokines, CXCL5 and/or CXCL8, and the overexpression of VEGFs in metastasis cancer cells.

4.3 Current HNSCC Cell Lines

Previously, we found that CXCL5 and CXCL8 were both highly overexpressed in HN12 versus HN4, 7.3 and 2.2 respectively. Current qRT-PCR analysis showed though only the overexpression of CXCL5 and no longer the overexpression of CXCL8. Expression levels of CXCL8 in HN12 are now comparable to the levels in HN4, which typically are very minimal. It is not clear but probable overtime and with continuous culture, for cells to be affected in their expression profile. We attempted to use an earlier stock of HN4 and HN12 cells in order to regain the overexpression of CXCL8, but it was unsuccessful. Therefore this study will determine the effect of overexpression of CXCL5, without the overexpression of CXCL8. CXCL8 expression levels will still be examined in the next steps, since it has been published to be an essential proangiogenic

chemokine for cell metastasis.

4.4 Pathway Inhibition

a) ***MAP kinase pathway***

Current experiments using qRT-PCR showed that inhibition of the MAPK pathway, caused an about 50% upregulation of angiogenic chemokine CXCL5. However, as we already know, these two cell lines originally hold 4.5 times difference of CXCL5 expression level, it is interesting that despite of original big gap of expression difference in this chemokine, MAP kinase inhibition resulted in same amount of relative reduction in its expression level. We suppose, in CXCL5 expression, there may be commonly shared CXCL5 expression machinery between HN4 and HN12, which utilize the MAP kinase pathway. Although additional co-existing molecular mechanism, which is not present in primary cell line HN4 can make metastatic cell line HN12 able to produce higher levels of CXCL5.

On the contrary, transcription level of CXCL8, which contains the same ELR(+) CXC sequence showed dramatic difference after the application of MAP kinase inhibitor. HN4 exhibited neglectable level of upregulation by the application of MAP kinase inhibitor, however, HN12 showed dramatic upregulation of CXCL8 transcription. Of note, as we described previously, we lost the high CXCL8 expression when compared to the original HN12 cell line. It is possible to say that upregulated MAP kinase activity caused this difference. More importantly, we observed the different chemokine expression when we inhibited same kinase pathway even if the chemokines belonged to same family.

These findings suggest a couple of possibilities for our cell lines. In between these HNSCC cell lines, they are using MAP kinase pathway for the regulation of these two chemokines expression but for the downregulation of its production. CXCL8 may possess different molecular machinery, which is not activated in HN4, which causes its low level of expression. In the latter presumption, we believe that these molecular switches can be highly upregulate if it exists or be activated in the primary cell line HN4. We presume because of a secondary modification introduced in this cell line HN12, it induced higher MAP kinase activation therefore suppressing its CXCL8 transcription.

Inhibition of MAPK resulted in an 80% upregulation of expression level of VEGF-C in the cell line HN12 but no detectable level of change in the primary cell line HN4. It is still too early to conclude the possible reason for this difference; however, previous research by other group mentioned the upregulation of VEGF-C by the presence of CXCL8 in HUVEC cell lines. If this is also applicable as a regulatory mechanism for the expression of CXCL8 in our HNSCC cell lines, upregulated CXCL8, which is induced by the inhibition of the MAP kinase pathway directly upregulated the transcription level of VEGF-C. This can be called an indirect upregulation mechanism by controlling MAP kinase activity. However, inhibition of the MAP kinase pathway showed an equal level of downregulation, 80%, in $VEGF_{165}$ expression, which is the most dominantly expressed among the VEGF-A splicing variants. This result may suggest that the VEGF-A is positively controlled by the MAP kinase activity but in between these two HNSCC cell lines, there may be no significant difference in the usage of its transcription machinery for $VEGF_{165}$.

b) ***AKT pathway***

Inhibition of the Akt pathway by the application of the inhibitor LY294002 was shown at final concentration 10 μM according to western blot analysis. At this concentration of inhibitor, qRT-PCR analysis showed that CXCL5 and CXCL8 were both downregulated in HN4 and HN12 cell lines. Even in the HN12 cell line, which normally shows highly upregulated transcription level of CXCL5 exhibited almost neglectable amount of change in CXCL5 transcription. In primary cell line HN4 showed 20-50% of downregulation of CXCL5 transcription, however the HN4 cell line is originally expresses almost no detectable level of CXCL5. Therefore, this change induced by this inhibitor is almost near to the detectable limitation, of note the amplitude of standard deviation was apparently few times bigger as compared to the other stable results. CXCL8 was downregulated in its transcription level by exposing to the Akt inhibitor. In both cell lines, downregulation of CXCL8 was almost the same at 40%. It may suggest that in between two different cell lines, they are sharing same machinery for the expression of CXCL8, which can upregulate its transcription by the activation of Akt pathway. By addition of the Akt inhibitor we observed a decrease in both proangiogenetic chemokines, CXCL5 and CXCL8.

Expression levels of VEGF-C were totally different in between these two cell lines. In HN4, VEGF-C transcription level was not affected by the inhibition of Akt pathway. However, HN12 cell line exhibited 100% upregulation in VEGF-C transcription. In $VEGF_{165}$ expression, HN12 cell line exhibited 50% downregulation in its transcription level, on the contrary, we observed 3 times upregulation in primary cell line HN4. Summarizing this data, at least we can predict several possibility in our HNSCC

cell line HN4 and HN12. VEGF-C transcription is found not to be under control of these two chemokines. In the metastatic cell line HN12, Akt is downregulating VEGF-C transcription.

In summary, analysis of our cell lines showed that inhibition of either MAPK or Akt pathway individually, both led to an increased levels of transcription of the lymphangiogenetic VEGF, VEGF-C, especially in HN12 cell line. Regardless of the expression levels of proangiogenic chemokines, CXCL5 or CXCL8, upregulated or downregulated, it resulted in an increase in VEGF-C expression. Therefore, VEGF-C expression may not be regulated by either CXCL5 or CXCL8. The inhibition of MAPK and Akt pathways however did not lead to an increase in all VEGFs. Expression levels of $VEGF_{165}$, the dominant VEGF-A isoform mainly responsible for angiogenesis, was downregulated in HN12. From these results, it can be concluded that VEGF-C and VEGF-A's transcription are regulated by different transcription machinery. We also conclude that regardless of an increase or decrease in chemokine expression, we still see an increase in VEGF-C and a decrease in VEGF-A expression. However, VEGF-C expression in HN12 is induced by the application of MAP kinase inhibitor, this could be a possible indirect induction induced by CXCL8 expression. Akt and MAPK were shown to downregulate VEGF-C expression, as well as signaling through CXCR2. Still there are many possibilities to be clarified by further experiments in this transcription-based study.

In the future to circumvent some of these problems, we may need to apply different methods for the suppression of these specific pathways, such as RNAi technology and/or shRNA based stable knockdown system for each independent kinase

pathway, to achieve more specific knockdown of kinase pathway. The application of inhibitors may also have a chance to circumvent causeing a risk of downregulating or upregulating unexpected pathway(s). However, it does not always certify that the use of RNAi based system sometimes has a chance to accompany with “off-target” effects, which can also downregulate unpredicted molecular target(s). Through this research, we picked up one important possibility that application of certain type of pharmacological inhibitor, which targets a specific kinase pathway, must be carefully used for anti-tumor purposes. Even if an inhibitor works specifically for the downregulation of an expected pathway, it may unexpectedly elicit the upregulation of certain unfavorable molecular expression directly or indirectly.

	CXCL5		CXCL8		VEGF-C	
MAPK	HN4 ↑ 50%	HN12 ↑ 50%	HN4 ↑ 20%	HN12 ↑ 180%	HN4 No change	HN12 ↑ 80%
Akt	HN4 ↓ 60%	HN12 ↓ 10%	HN4 ↓ 40%	HN12 ↓ 40%	HN4 No change	HN12 ↑ 100%

Table 4. Summary of Inhibition

c) ***p38 MAP kinase pathway***

We also attempted many times to downregulate p38 MAP kinase pathway in our cell lines HN4 and HN12, since this has been shown to be a predominate pathway in both chemokines and VEGF-C expression according to several other's research. However, to our disappointment, freshly prepared two different p38 inhibitors as well as various different conditions, we were unable to successfully downregulate the activation of p38 MAP kinase. Although, we could successfully confirm downregulation of p38 MAP kinase pathway in other cell lines, such as 293T or NIH3T3 cell lines.

4.5 Inhibition of CXCR2

CXCR2, a G-protein coupled receptor, is a specific chemokine receptor for CXCL5 and CXCL8. A competitive inhibitor of CXCR2 was used to block the activation of this receptor. Using qRT-PCR analysis, we examined the resultant expression of VEGF-C and VEGF-A due to CXCR2 inhibition. Upon inhibition of CXCR2, we observed in the HN12 cell line, an upregulated transcription of VEGF-C, 150%, and a 20% reduction in $VEGF_{165}$ expression. This is quite similar to the previous output obtained through the inhibition of chemokines CXCL5 and CXCL8 expression by using the Akt inhibitor, which exhibited a 100% upregulation in VEGF-C, but a 50% downregulation in $VEGF_{165}$. This similarity may suggest possible presence of signaling pathway, which starts from CXCR2 via Akt signaling pathway for the negative regulation of VEGF-C expression.

4.6 Limitations of HNSCC Model System

The HNSCC model system that is used in this study has limitations that must be considered. Even though these cell lines were derived from one male patient that limits the genetic background variation, it does not completely eliminate it. Between these cell lines numerous numbers of genes, were found to upregulated or downregulated based on cDNA microarray analysis. Any number of these genes could impact the genetic background and affect the molecules and regulations examined in this study. Also, as we already mentioned above, pharmacological inhibitor based kinase suppression could also cause secondary effects on other molecular expression profiles directly or indirectly and it is inevitable with any type of pharmacological inhibitor.

In vitro studies also have their innate limitations. This study only involves one specific tissue, which has been isolated outside the body. Similar *in vivo* experiments could reveal different results due to multiple factors present that could interact and change the conditions of this study. Our current results though are a good starting point to continue investigation of the role of chemokines and VEGFs expression in HNSCC.

4.7 Future Studies

The current study has begun to sort out the expression and regulation of chemokines and VEGFs in HNSCC. There are still many unanswered questions about the role these molecules play in HNSCC. Of course there are additional experiments which should be done to continue sorting out the regulation of these chemokines and VEGFs. First, determining a method to knockdown p38 MAP kinase in these cell lines would be beneficial since this is a predominant pathway in both chemokine and VEGF

signaling. Although the pharmacological inhibitors that were used seemed to successfully knockdown specific kinase pathways, they can lead to unseen adverse effects. Other knockdown systems should be tested such as shRNA or RNAi mediated system, to see if the results are the same. Transfecting these cell line with constitutively active or dominant negative forms of the kinase could also be helpful. The use of an *in vivo* model could be supportive and reinforce our current findings, as well as investigating these results in other cancer cell lines.

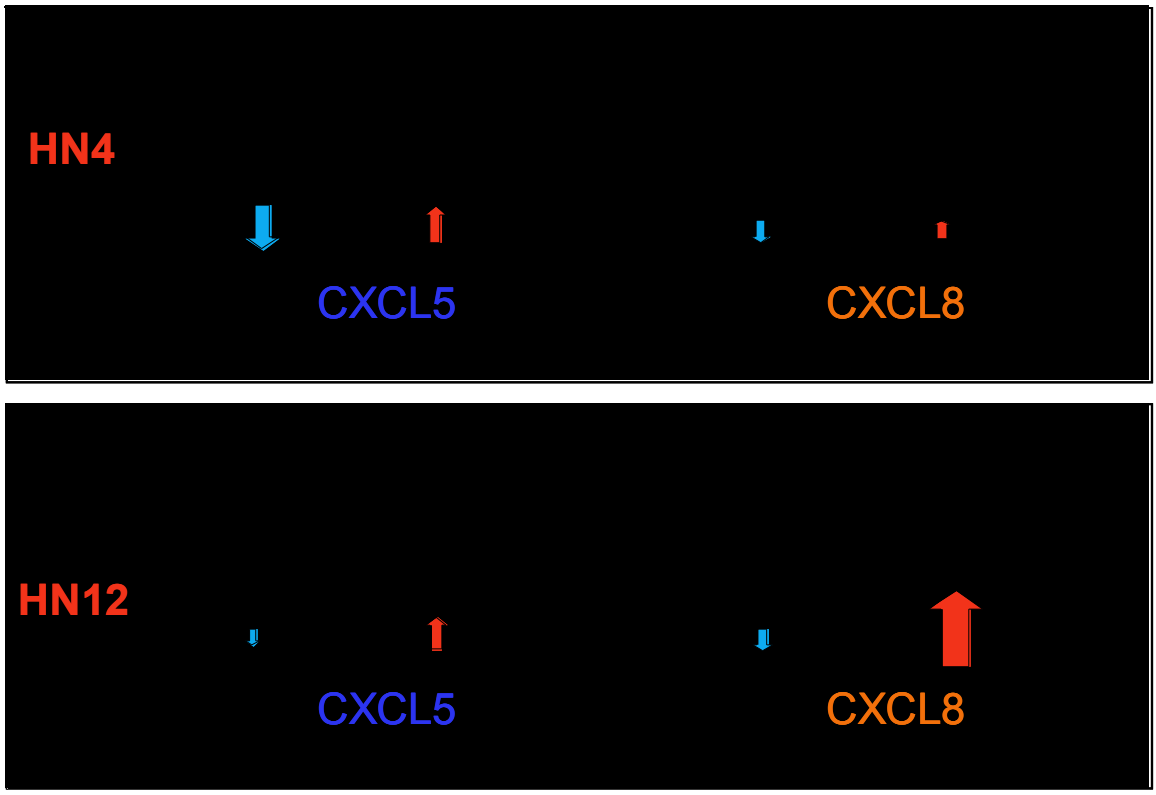

Figure 16. Summary of Chemokine Regulation. The Akt pathway was shown to upregulate the transcription of CXCL5 and CXCL8 in both HN4 and HN12. The MAPK pathway was shown to cause a downregulation of CXCL5 and CXCL8 in both HN4 and HN12.

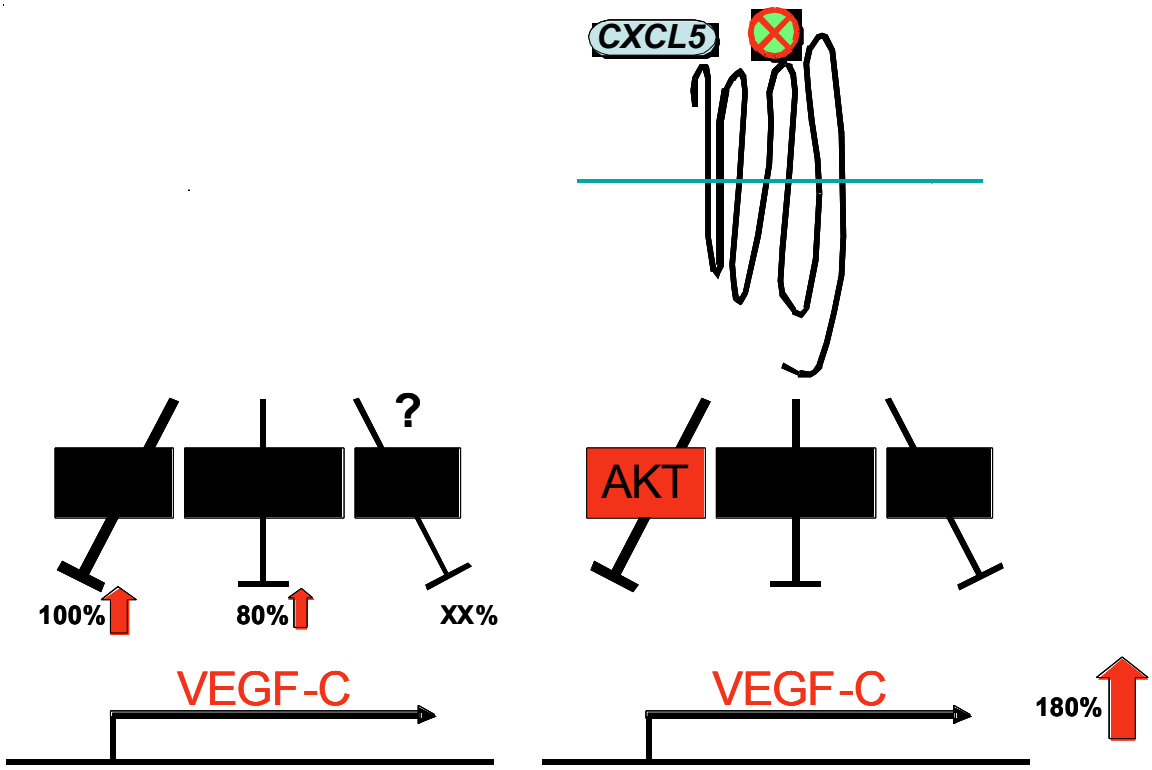

Figure 17. Summary of VEGF-C Regulation. Inhibition of the Akt or MAPK pathway, either individually or through the inhibition of CXCR2 causes an upregulation of VEGF-C. These pathways were shown to downregulate the VEGF-C expression.

Literature Cited

Addison Christina, Daniel Thomas, Burdick Marie, Liu Hua, Ehlert Jan, Xue Ying Ying, Buechi Linda, Walz Alfred, Richmond Ann, Strieter Robert. The CXC Chemokine Receptor 2, CXCR2, Is the Putative Receptor for ELR+ CXC Chemokine-Induced Angiogenic Activity. *The Journal of Immunology*: 5269-5277, 2000.

American Cancer Society. (2009). Cancer Facts and Figures. Website: www.cancer.org

Begley Lesa, Kasina, Sathish, Mehra Rohit, Adsule Shreelekha, Admon Andrew, Lonigro Robert, Chinnaiyan Arul, Macoska Jill. CXCL5 Promotes Prostate Cancer Progression. *Neoplasia* 10 (3): 244-254, March 2008.

Christofakis Emil. Effects of CXCL8 Overexpression on Tumor Cell Prolifreation and Migration in an HNSCC Cell Model. 2007.

Deb Swati Palit, Deb Sumtria. p53 protocols. Methods in Molecular Biology Volume 234. Humana Press. 2003.

Delcourt Nicolas, Bockert Joel, Marin Philippe. GPCR-jacking: from a new route in RTK signaling to a new concept in GPCR activation. *Trends in Pharmacological Sciences* 28 (12): 602-607, 2007.

Eccles Suzanne, Paon Lenaic, Sleeman Johnathan. Lymphatic metastasis in breast cancer: importance and new insights into cellular and molecular mechanisms. *Clinical Exp Metastasis* 24: 619-636, 2007.

George Mark, Tutton Matthew, Janssen Frank, Arnaout Abed, Abulafi A. Muti, Eccles Suzanne, Swift R. Ian. VEGF-A, VEGF-C, and VEGF-D in Colorectal Cancer Progression. *Neoplasia* 3 (5): 420-427, 2001.

Kimura Hideo, Weisz Alessandro, Kurashima Yukiko, Hashimoto Kouichi, Ogura Tsutomu, D'Acquisto Fulvio, Addeo Raffaelo, Makuuchi Masatocshi, Esumi Hiroyasu. Hypoxia response element of the human vascular endothelial growth factor gene mediates transcriptional regulation by nitric oxide: control of hypoxia-inducible factor-1 activity of nitric oxide. *Blood* 95 (1): 189-197, January 2000.

Lodish Harvey, Berk Arnold, Kaiser Chris, Kriger Monty, Scott Matthew, Bretscher Anthony, Ploegh Hidde, Matsudaira Paul. Molecular Cell Biology. Sixth Edition. W.H. Freedman Company. 2008.

Martin, Daniel, Galisteo Rebeca, Gutkind J. Silvio. CXCL8/IL8 Stimulates VEGF Expression and the Autocrine Activation of VEGFR2 in Endothelial Cells by Activating NFkB through the CBM (CARMA3/BCL10/MATL1) Complex. *The Journal of Biological Chemistry*. 284(10):6038-42. March 2009.

Mehrad Borna, Keane Michael, Strieter Robert. Chemokines as mediators of angiogenesis. *Chemokines in Vascular Biology*. Thromb Haemost, 97: 755-767, 2007.

Miyazaki Hiroshi, Patel Vyomesh, Wang Huixin, Edmund Ryan, Gutkind J. Silvio, Yeudall Andrew. Down-regulation of CXCL5 Inhibits Squamous Carcinogenesis. *Cancer Research* 66 (8): 4279-4284, 2006.

Miyazaki Hiroshi, Patel Vyomesh, Wang Huixin, Ensley John, Gutkind J. Silvio, Yeudall Andrew. Growth factor-sensitive molecular targets identified in primary and metastatic head and neck squamous cell carcinoma using microarray analysis. *Oral Oncology* 42: 240-256, 2006.

McMahon Steve, Chen Amy. Head and Neck Cancer. *Cancer and Metastasis Reviews* 22: 21-24, 2003.

Neuchrist, Csilla, Erovia Bohan, Handisurya Allesandra, Fishcer Michael, Steiner Georg, Hollemann David, Gedlicka Claudia, Saaristo A, Burian Martin. Vascular Endothelial Growth Factor C and Vascular Endothelial Growth Factor Receptor 3 Expression in Squamous Cell Carcinomas of the Head and Neck. *Head and Neck* 25: 464-474, 2003.

Ninck Simon, Reisser Christoph, Dyckhoff Gerhard, Helmke Burkhard, Bauer Harald, Herold-Mende Christel. Expression Profiles of Angiogenic Growth Factors in Squamous Cell Carcinomas of the Head and Neck. *Int J. Cancer* 106: 34-44, 2003.

O'Harye Morgan, Salanga Catherina, Handel Tracy, Allen Samantha. Chemokines and cancer; migration, intracellular signaling and intercellular communication in the microenvironment. *Biochem J.* 409: 635-649, 2008.

Paccione Rachel, Miyazaki Hiroshi, Patel Vyomesh, Waseem Ahmad, Gutkind J. Silvio, Zehner Zendra, Yeudall Andrew. Keratin down-regulation in vimentin-positive cancer cells is reversible by vimentin RNA interference, which inhibits growth and motility. *Molecular Cancer Therapeutics* 7 (9): 2894-2903, September 2008.

Petreaca Melissa, Yao Min, Liu Yan, DeFea Kathryn, Martins-Green Manuela. Transactivation of Vascular Endothelial Growth Factors Receptor-2 by Interleukin-8 (IL-8/CXCL8) Is Required for IL-8/CXCL8-induced Endothelial Permeability. *Molecular Biology of the Cell* 18: 5014-5023, December 2007.

Piiper A, Zeuzem S. Receptor Tyrosine Kinases are Signaling Intermediates of G Protein Coupled Receptors. *Current Pharmaceutical Design* 10: 3539-3545, 2004.

Raman Dayanidhi, Baugher Paige, Thu Yee Mon, Richmond Ann. Role of chemokines in tumor growth. *Cancer Letters* 256: 137-165, 2007.

Sabbah Michele, Emami Shahin, Redeuilh Gerard, Julien Sylvia, Prevost Gregoire, Zimber Amazia, Ouelaa Radia, Bracke Marc, DeWever Olivier, Gespach Christian.

Molecular signature and therapeutic perspective of the epithetial-to-mesenchymal transitions in epithelial cancers. *Drug Resistance Updates* 11: 123-151, 2008.

Schruefer Ruth, Lutze Nicola, Schymeinsky Jurgen, Walzog Barbara. Human neutrophils promote angiogenesis by a paracrine feedforward mechanism involving endothelial interleukin-8. *Am J Physiol Heart Circ Phyciol* 288: 1186-1192, 2005.

Singh Seema, Sadanandam Anguraj, Singh Rakesh. Chemokines in tumor angiogenesis and metastasis. *Cancer Metastasis Review* 26: 453-467, 2007.

South ST, Whitby H, Maxwell T, Aston E, Brothman AT, Carey JC. Co-occurrence of 4p16.3 deletions with both paternal and maternal duplications of 11p15: modification of the Wolf-Hirschhorn syndrome phenotype by genetic alterations predicted to result in either a Beckwith-Wiedemann or Russell-Silver phenotype. *American Journal of Medical Genetics*. 146A(20)2691-7. October 15 2008.

Sun Hongxia, Chung Wen-Cheng, Ryu Seung-Hee, Ju Zhenlin, Tran Hai, Kim Edward, Kurie Johnathan, Koo Ja Seok. Cyclic AMP-Responsive Elements Binding Protein- and Nucl

Tammela Tuomas, Zarkada Georgia, Wallgard Elisabet, Murtomaki Aino, Suchting Steven, Wirzeninus Maria, Waltari Markia, Hellstrom Mats, Schomber Tibor, Peltonen Reetta, Freitas Caterina, Duarte Antonio, Isoniemi Helena, Laakkonen Pirjo, Christofori Gerhard, Yla-Herttuala Seppo, Shibuya Masabumi, Pytowshi Bronislaw, Eichmann Anne, Betsholtz Christer, Alitaol Kari. Blocking VEGFR-3 suppresses angiogenic sprouting and vascualar network formation. *Nature* 454: 656-662, July 31, 2008.

Thomas Sufi Mary, Bhola Neil E, Zhang Qing, Contrucci Sarah, Wentzel Abbey, Freilino Maria, Gooding William, Siegfried Jill, Chan Daniel, Grandis Jennifer Rubin. Cross-talk between G Protein-Coupled Receptor and Epidermal Growth Factor Receptor Signaling Pathways Contributes to Growth and Invasion of Head and Neck Squamous Cell Carcinomas. *Cancer Research* 66 (24): 11831-11839, December 15, 2006.

Tong Meng, Llyod Brandon, Pei Ping, Mallery Susan. Human Head and Neck Squamous Cell Carcinoma Cells Are Both Targets and Effectors for the Angiogenic Cytokine, VEGF. *Journal of Cellular Biochemistry* 105: 1202-1210, 2008.

Trevino Jose, Summy Justin, Gray Michael, Nilsson Monique, Lesslie Donald, Baker Cheryl, Gallick Gary. Expression and Activity of Src Regulated Interleukin-8 Expression in Pancreatic Adenocarcinoma Cells: Implications for Angiogenesis. *Cancer Research*; 65: (16) 7214-7222, August 15, 2005.

Tsai Pei-Wen, Shiah Shine-Gwo, Lin Ming-Tsan, Wu Cheng-Wen, Kuo Min-Liang. Up-regulation of Vascular Endothelial Growth Factor C in Breast Cancer Cells by Heregulin-b1. *The Journal of Biological Chemistry* 278 (8): 5750-5759, 2003.

Waugh David, Wilson Katherine. The Interleukin-8 Pathway in Cancer. *Clinical Cancer Research* 14 (21): 6735-6740, November 1, 2008.

Yeudall Andrew, Miyazaki Hiroshi, Ensley John, Cardinali Massimo, Gutkind J. Silvio, Patel Vyomesh. Uncoupling of epidermal growth factor-dependent proliferation and invasion in a model of squamous carcinoma progression. *Oral Oncology* 41: 698-708, 2005.

Zhang Qian, Guo Ruolin, Lu Yan, Zhao Lan, Zhou Quan, Schwarz Edward, Huang Jing, Chen Di, Jin Zheng-Gen, Boyce Brendan, Xing Lianping. VEGF-C, a Lymphatic Growth Factor, Is a RANKL Target Gene in Osteoclasts that Enhances Osteoclastic Bone Resorption through an Autocrine Mechanism. *The Journal of Biological Chemistry* 283 (19): 13491-13499, May 9, 2008.

Zlotnik Albert, Yoshie Osamu. Chemokines: A New Classification System and Their Role in Immunity. *Immunity* 12: 121-127. February 2000.